



The influence of environmental variability on the biogeography of coccolithophores and diatoms in the Great Calcite Belt

Helen E. K. Smith^{1,2}, Alex J. Poulton^{1,a}, Rebecca Garley³, Jason Hopkins⁴, Laura C. Lubelczyk⁴, Dave T. Drapeau⁴, Sara Rauschenberg⁴, Ben S. Twining⁴, Nicholas R. Bates^{2,3}, and William M. Balch⁴

¹National Oceanography Centre, European Way, Southampton, SO14 3ZH, UK

²Ocean and Earth Science, National Oceanography Centre Southampton, University of Southampton, Southampton, SO14 3ZH, UK

³Bermuda Institute of Ocean Sciences, 17 Biological Station, Ferry Reach, St. George's GE 01, Bermuda

⁴Bigelow Laboratory for Ocean Sciences, 60 Bigelow Drive, P.O. Box 380, East Boothbay, Maine 04544, USA

^apresently at: The Lyell Centre, Heriot-Watt University, Edinburgh, EH14 4AS, UK

Correspondence to: Helen E. K. Smith (helen.eksmith@gmail.com)

Received: 27 March 2017 – Discussion started: 13 April 2017

Revised: 24 August 2017 – Accepted: 20 September 2017 – Published: 7 November 2017

Abstract. The Great Calcite Belt (GCB) of the Southern Ocean is a region of elevated summertime upper ocean calcite concentration derived from coccolithophores, despite the region being known for its diatom predominance. The overlap of two major phytoplankton groups, coccolithophores and diatoms, in the dynamic frontal systems characteristic of this region provides an ideal setting to study environmental influences on the distribution of different species within these taxonomic groups. Samples for phytoplankton enumeration were collected from the upper mixed layer (30 m) during two cruises, the first to the South Atlantic sector (January–February 2011; 60° W–15° E and 36–60° S) and the second in the South Indian sector (February–March 2012; 40–120° E and 36–60° S). The species composition of coccolithophores and diatoms was examined using scanning electron microscopy at 27 stations across the Subtropical, Polar, and Subantarctic fronts. The influence of environmental parameters, such as sea surface temperature (SST), salinity, carbonate chemistry (pH, partial pressure of CO₂ (*p*CO₂), alkalinity, dissolved inorganic carbon), macronutrients (nitrate + nitrite, phosphate, silicic acid, ammonia), and mixed layer average irradiance, on species composition across the GCB was assessed statistically. Nanophytoplankton (cells 2–20 μm) were the numerically abundant size group of biomineralizing phytoplankton across the GCB, with the coccolithophore *Emiliania huxleyi* and diatoms *Fragilariopsis nana*, *F. pseudonana*, and *Pseudo-nitzschia* spp. as the most

numerically dominant and widely distributed. A combination of SST, macronutrient concentrations, and *p*CO₂ provided the best statistical descriptors of the biogeographic variability in biomineralizing species composition between stations. *Emiliania huxleyi* occurred in silicic acid-depleted waters between the Subantarctic Front and the Polar Front, a favorable environment for this species after spring diatom blooms remove silicic acid. Multivariate statistics identified a combination of carbonate chemistry and macronutrients, covarying with temperature, as the dominant drivers of biomineralizing nanoplankton in the GCB sector of the Southern Ocean.

1 Introduction

The Great Calcite Belt (GCB), defined as an elevated particulate inorganic carbon (PIC) feature occurring alongside seasonally elevated chlorophyll *a* in austral spring and summer in the Southern Ocean (Fig. 1; Balch et al., 2005), plays an important role in climate fluctuations (Sarmiento et al., 1998, 2004), accounting for over 60 % of the Southern Ocean area (30–60° S; Balch et al., 2011). The region between 30 and 50° S has the highest uptake of anthropogenic carbon dioxide (CO₂) alongside the North Atlantic and North Pacific oceans (Sabine et al., 2004). Our knowledge of the impact of interacting environmental influences on phytoplankton distribution in the Southern Ocean is limited. For example, we do

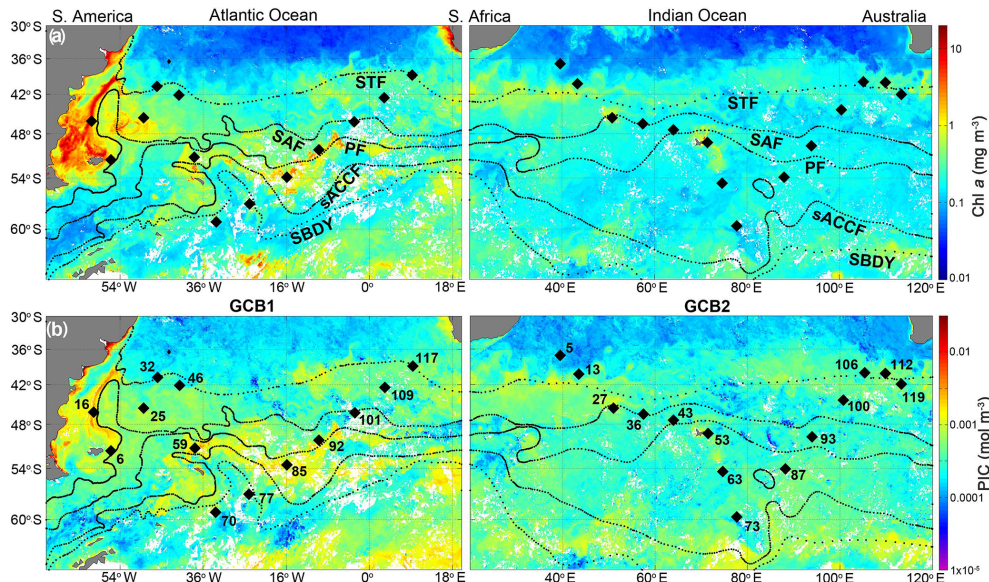


Figure 1. Rolling 32-day composite from MODIS Aqua for both (a) chlorophyll *a* (mg m^{-3}) and (b) PIC (mol m^{-3}) for the South Atlantic sector (17 January to 17 February 2011) and the South Indian sector (18 February to 20 March 2012). Station number identifiers and averaged positions of fronts as defined by Orsi et al. (1995) are superimposed: Subtropical Front (STF), Subantarctic Front (SAF), Polar Front (PF), Southern Antarctic Circumpolar Current Front (SACCF), and southern boundary (SBDY).

not yet fully understand how light and iron availability or temperature and pH interact to control phytoplankton biogeography (Boyd et al., 2010, 2012; Charalampopoulou et al., 2016). Hence, if model parameterizations are to improve (Boyd and Newton, 1999) to provide accurate predictions of biogeochemical change, a multivariate understanding of the full suite of environmental drivers is required.

The Southern Ocean has often been considered as a microplankton-dominated (20–200 μm) system with phytoplankton blooms dominated by large diatoms and *Phaeocystis* sp. (e.g., Bathmann et al., 1997; Poulton et al., 2007; Boyd, 2002). However, since the identification of the GCB as a consistent feature (Balch et al., 2005, 2016) and the recognition of picoplankton (< 2 μm) and nanoplankton (2–20 μm) importance in high-nutrient, low-chlorophyll (HNLC) waters (Barber and Hiscock, 2006), the dynamics of small (bio)mineralizing plankton and their export need to be acknowledged. The two dominant biomineralizing phytoplankton groups in the GCB are coccolithophores and diatoms. Coccolithophores are generally found north of the PF (e.g., Mohan et al., 2008), though *Emiliania huxleyi* has been observed as far south as 58° S in the Scotia Sea (Holligan et al., 2010), at 61° S across Drake Passage (Charalampopoulou et al., 2016), and at 65° S south of Australia (Cubillos et al., 2007).

Diatoms are present throughout the GCB, with the Polar Front marking a strong divide between different size fractions (Froneman et al., 1995). North of the PF, small diatom species, such as *Pseudo-nitzschia* spp. and *Thalassiosira* spp., tend to dominate numerically, whereas large di-

atoms with higher silicic acid requirements (e.g., *Fragilariopsis kerguelensis*) are generally more abundant south of the PF (Froneman et al., 1995). High abundances of nanoplankton (coccolithophores, small diatoms, chrysophytes) have also been observed on the Patagonian Shelf (Poulton et al., 2013) and in the Scotia Sea (Hinz et al., 2012). Currently, few studies incorporate small biomineralizing phytoplankton to species level (e.g., Froneman et al., 1995; Bathmann et al., 1997; Poulton et al., 2007; Hinz et al., 2012). Rather, the focus has often been on the larger and noncalcifying species in the Southern Ocean due to sample preservation issues (i.e., acidified Lugol's solution dissolves calcite, and light microscopy restricts accurate identification to cells > 10 μm ; Hinz et al., 2012). In the context of climate change and future ecosystem function, the distribution of biomineralizing phytoplankton is important to define when considering phytoplankton interactions with carbonate chemistry (e.g., Langer et al., 2006; Tortell et al., 2008) and ocean biogeochemistry (e.g., Baines et al., 2010; Assmy et al., 2013; Poulton et al., 2013).

The GCB spans the major Southern Ocean circumpolar fronts (Fig. 1a): the Subantarctic Front (SAF), the Polar Front (PF), the Southern Antarctic Circumpolar Current Front (SACCF), and occasionally the southern boundary of the Antarctic Circumpolar Current (ACC; see Tsuchiya et al., 1994; Orsi et al., 1995; Belkin and Gordon, 1996). The Subtropical Front (STF; at approximately 10 °C) acts as the northern boundary of the GCB and is associated with a sharp increase in PIC southwards (Balch et al., 2011). These fronts divide distinct environmental and biogeochem-

ical zones, making the GCB an ideal study area to examine controls on phytoplankton communities in the open ocean (Boyd, 2002; Boyd et al., 2010). A high PIC concentration observed in the GCB ($1 \mu\text{mol PIC L}^{-1}$) compared to the global average ($0.2 \mu\text{mol PIC L}^{-1}$) and significant quantities of detached *E. huxleyi* coccoliths (in concentrations $> 20\,000$ coccoliths mL^{-1} ; Balch et al., 2011) both characterize the GCB. The GCB is clearly observed in satellite imagery (e.g., Balch et al., 2005; Fig. 1b) spanning from the Patagonian Shelf (Signorini et al., 2006; Painter et al., 2010) across the Atlantic, Indian, and Pacific oceans and completing Antarctic circumnavigation via the Drake Passage.

GCB waters are characterized as high nitrate, low silicate, and low chlorophyll (HNLSiLC; e.g., Dugdale et al., 1995; Leblanc et al., 2005; Moore et al., 2007; Le Moigne et al., 2013), in which dissolved iron (dFe) is considered an important control on microplankton ($> 20 \mu\text{m}$) growth (e.g., Martin et al., 1990; Gall et al., 2001; Venables and Moore, 2010). Sea surface temperature (SST) gradients are a driving factor behind phytoplankton biogeography and community composition (Raven and Geider, 1988; Boyd et al., 2010). The influence of environmental gradients on biomineralizing phytoplankton in the Scotia Sea and the Drake Passage has also been assessed (Hinz et al., 2012; Charalampopoulou et al., 2016). However, the controls on the distribution of biomineralizing nanoplankton are yet to be established for the wider Southern Ocean and GCB. Previous studies have predominantly focused on a single environmental factor (e.g., Eynaud et al., 1999) or combinations of temperature, light, macronutrients, and dFe (e.g., Poulton et al., 2007; Mohan et al., 2008; Balch et al., 2016) to explain phytoplankton distribution. The inclusion of carbonate chemistry as an influence on phytoplankton biogeography is a relatively recent development (e.g., Charalampopoulou et al., 2011, 2016; Hinz et al., 2012; Poulton et al., 2014; Marañón et al., 2016). Furthermore, natural variability in ocean carbonate chemistry and the resulting impact on in situ phytoplankton populations remains a significant issue when considering the impact of future climate change.

An increasing concentration of dissolved CO_2 in the oceans is resulting in “ocean acidification” via a decrease in ocean pH (Caldeira and Wickett, 2003). In the high latitudes where colder waters enhance the solubility of CO_2 and reduce the saturation state of calcite, there may be potential detrimental effects on calcifying phytoplankton (Doney et al., 2009). However, this may be species specific (Langer et al., 2006) or even strain specific (Langer et al., 2011), showing an optimum response when the opposing influences of pH and bicarbonate are considered in a substrate-inhibitor concept (Bach et al., 2015). The response of noncalcifiers (e.g., diatoms) to ocean acidification is a greater unknown but is no less important given their ~ 40 to 50% contribution to global primary production (e.g., Tréguer et al., 1995; Sarthou et al., 2005). Tortell et al. (2008) observed a switch from small to large diatom species with increasing CO_2 , in-

dicating a potential change in future community structure. Large phytoplankton species ($> 50 \mu\text{m}$) may also have physiological traits to withstand changes in ocean chemistry over smaller-celled ($< 50 \mu\text{m}$) species (Flynn et al., 2012) and potentially be less susceptible to grazing pressure (Assmy et al., 2013). Alternatively, there may be a shift towards small phytoplankton groups due to the expansion of low-nutrient subtropical regions (Bopp et al., 2001, 2005). The response of Southern Ocean phytoplankton biogeography to future climate conditions, including ocean acidification, is complex (e.g., Charalampopoulou et al., 2016; Petrou et al., 2016; Deppeler and Davidson, 2017) and therefore understanding existing relationships between in situ phytoplankton communities and ocean chemistry is an important stepping stone for predicting future changes.

Here, we assess the distribution of coccolithophore and diatom species in relation to the environmental conditions encountered across the GCB. Diatom and coccolithophore cell abundances were obtained from analysis of scanning electron microscopy (SEM) images, and their distribution was statistically assessed in relation to SST, salinity, mixed layer average irradiance, macronutrients, and carbonate chemistry. Herein, we examine the spatial differences within the biomineralizing phytoplankton in the GCB, the main environmental drivers behind their biogeographic variability, and the potential effects of future carbonate chemistry perturbations.

2 Methods

2.1 Sampling area

Two cruises were undertaken in the GCB during 2011 and 2012 (<http://www.bco-dmo.org/project/473206>). The Atlantic sector of the Southern Ocean (GCB1) was sampled from 11 January to 16 February 2011 onboard the R/V *Melville* between Punta Arenas, Chile and Cape Town, South Africa (Balch et al., 2016; Fig. 1). The Indian sector of the Southern Ocean (GCB2) was sampled from 18 February to 20 March 2012 onboard the R/V *Revelle* between Durban, South Africa and Fremantle, Australia (Fig. 1). Water samples were taken at 27 stations across a latitudinal gradient ranging from 38 to 60° S and a longitudinal gradient ranging from 60° W to 120° E during the GCB cruises, which enabled sampling of the major oceanographic features of this region.

2.2 Physiochemical environmental conditions

Water samples were collected from the upper 30 m of the water column using a Niskin bottle rosette and CTD profiler for sea surface temperature, salinity, chlorophyll *a* (Chl *a*), nitrate plus nitrite (NO_x), ammonia (NH_4), phosphate (PO_4), silicic acid ($\text{Si}(\text{OH})_4$), and carbonate chemistry. Nutrient analyses of NO_x , PO_4 , $\text{Si}(\text{OH})_4$, and NH_4 were run on a Seal Analytical continuous-flow AutoAnalyzer 3, while salinity

was determined using a single Guildline Autosol 8400B stock salinometer (S/N 69-180). Chlorophyll *a* was sampled in triplicate following Joint Global Ocean Flux Study (JGOFS; Knap et al., 1996) protocols. Mixed layer depths were calculated from processed CTD data by applying a criteria of a 0.02 kg m^{-3} density change from the 5 m value (Arrigo et al., 1998). Daily photosynthetically active radiation (PAR, $\text{mol PAR m}^{-2} \text{ d}^{-1}$) was estimated from 8-day composite Aqua MODIS data from the closest time and latitude–longitude point (averages were taken where necessary). Mixed layer average irradiance (\bar{E}_{MLD}) was calculated from daily PAR following Poulton et al. (2011).

Water samples were collected for total dissolved inorganic carbon (C_{T}) and total alkalinity (A_{T}) following standardized methods and analyzed using a Versatile Instrument for the Determination of Titration Alkalinity (VINDTA) with a precision and accuracy of $\pm 1 \mu\text{mol kg}^{-1}$ (Bates et al., 1996, 2012). The remaining carbonate chemistry parameters were calculated from the C_{T} and A_{T} values using CO₂SYS (Lewis and Wallace, 1998) and CO₂calc (Robbins et al., 2010) with the carbonic acid dissociation constants of Mehrbach et al. (1973) refitted by Dickson and Millero (1987). This includes computation of the saturation state (Ω) for calcite (i.e., Ω_{calcite}).

2.3 Phytoplankton enumeration

Samples for biomineralizing phytoplankton community structure were taken from the upper 30 m of the water column. One-liter seawater samples were collected and pre-filtered through a 200 μm mesh to remove any large zooplankton. Seawater samples were gently filtered through a 25 mm, 0.8 μm Whatman[®] polycarbonate filter placed over a 200 μm backing mesh to ensure an even distribution of cells across the filter. Filters were rinsed with $\sim 5 \text{ mL}$ of potassium tetraborate (0.02 M) buffer solution ($\text{pH} = 8.5$) to prevent salt crystal growth and PIC dissolution, air-dried, and stored in petri slides in the dark with a desiccant until further analysis.

To identify coccolithophores to the species level, each sample was imaged using the SEM methodology of Charalampopoulou et al. (2011). A central portion of each filter was cut out and gold coated, and 225 photographs were taken at a magnification of $5000 \times$ (equivalent to $\sim 1 \text{ mm}^2$; GCB1) or $3000 \times$ ($\sim 2.5 \text{ mm}^2$; GCB2) using a Leo 1450VP SEM (Carl Zeiss, Germany). Detached coccoliths and whole coccolithophore cells (coccospheres) were identified following Young et al. (2003). Diatoms and other recognizable protists were identified following Hasle and Syvertsen (1997) and Scott and Marchant (2005). Where a confident species level identification was not possible, cells were assigned to the level of genera (e.g., *Chaetoceros* spp. or *Pappamonas* sp.). Each species identified was enumerated using the free-ware ImageJ (v1.44o) for all 225 images or until 300 cells (or coccoliths) were counted. A minimum of 10 random images was picked for enumeration when species were in high abun-

dance ($> 1000 \text{ cells mL}^{-1}$). The abundance of each species was calculated following Eq. (1):

$$\text{Cells mL}^{-1} = (C \times F/A)/V, \quad (1)$$

where C is the total number of cells (or coccoliths) counted, A is the area investigated (mm^2), F is the total filter area (mm^2), and V is the volume filtered (mL).

2.4 Statistical analysis

Multivariate statistics (PRIMER-E v.6.1.6; Clarke and Gorley, 2006) were used to examine spatial changes in coccolithophore and diatom abundance, species distribution, and the influence of environmental variability on biogeography (e.g., Charalampopoulou et al., 2011, 2016). Environmental data were initially assessed for skewness, most likely due to strong chemical gradients across fronts. Heavily left-skewed variables (NO_x , silicic acid, and NH_4) were $\log(V + 0.1)$ transformed to reduce skewness and stabilize variance. Other environmental data, including SST, salinity, \bar{E}_{MLD} , NO_x , silicic acid, NH_4 , pH, $p\text{CO}_2$, and Ω_{calcite} , were then normalized to a mean of zero and a standard deviation of 1, and Euclidean distance was then used to determine spatial changes in these parameters. A principal component analysis (PCA) was used to simplify environmental variability by combining the more closely correlated variables and the relative influence of the environmental variables within the data (Clarke, 1993; Clarke and Warwick, 2001; Clarke and Gorley, 2006).

Coccolithophore and diatom species diversity was assessed as the total number of species (S) and Pielou's evenness index (J'), which assesses how evenly the count data were distributed between the different species present (before further statistical analysis). Species with cell counts of less than 1 cell mL^{-1} and/or consistently representing less than 1 % of the total cell abundance were excluded from multivariate statistical analysis to reduce the influence of rare species. Analysis of coccolithophore and diatom community structure was carried out on standardized and square-root-transformed cell abundance (to reduce the influence of numerically abundant species) using a Bray–Curtis similarity matrix. Bray–Curtis similarity describes the percentage of similarity (or dissimilarity) between different communities according to their relative species composition. To identify which stations had a statistically similar biomineralizing phytoplankton community across the GCB, a SIMPROF routine (1000 permutations, 5 % significance level) was applied to the Bray–Curtis similarity matrix. SIMPROF identifies, based on pairwise tests of the calculated Bray–Curtis percentage similarity, whether the similarities between samples are smaller and/or larger than those expected by chance and groups those that are statistically distinct (Clarke et al., 2008). The phytoplankton species driving the differences between the groups were identified through a SIMPER routine and presented using nonmetric multidimensional scaling (nMDS; Clarke, 1993; Clarke and Warwick, 2001; Clarke

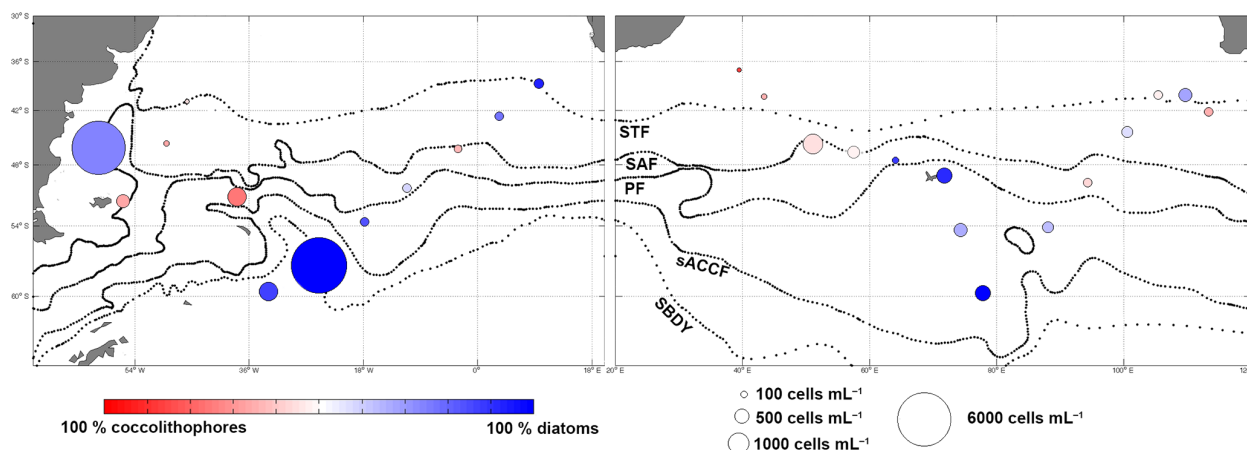


Figure 2. Coccolithophore and diatom abundance and dominance information. The area of the circles denotes abundance, while the shading denotes percentage contribution of each phytoplankton group; red denotes coccolithophore dominance and blue denotes diatom dominance. Fronts are defined as in Fig. 1.

and Gorley, 2006). SIMPER allows for the statistical identification of which species are primarily responsible for differences between groups of samples and breaks down the Bray–Curtis similarity into individual species contributions.

A BEST routine was applied to environmental and plankton data to determine the combination of environmental variables that “best” described the variability in coccolithophores and diatoms across the GCB. The BEST routine statistically searches for relationships between the biotic and abiotic patterns and to identify which environmental variable(s) explained most of the variation in species distribution. Spearman’s rank correlations were used to further investigate the relationship between the key environmental variables identified in the BEST routine and selected coccolithophore and diatom species.

3 Results

3.1 General oceanography

The GCB cruises crossed various biogeochemical gradients associated with the Antarctic Circumpolar Current (ACC) fronts and subcurrents, with most parameters following a recognizable latitudinal (or zonal) pattern. The position of the oceanic fronts referred to in the text relates to those defined in Fig. 1 (see also Balch et al., 2016). Sea surface temperature decreased southwards from 21 °C north of the STF to 1.1 °C close to 60° S (Table 1). The calcite saturation state (Ω_{calcite}) decreased from 5.2 north of the subtropical front to 2.6 close to 60° S (Table 1). Macronutrient concentrations generally increased southwards with a distinct divide across the SAF. NO_x ranged from below detection limits ($< 0.1 \mu\text{M}$) to as high as 28 μM , with higher concentrations generally south of the Subantarctic Front ($> 12 \mu\text{M}$) and lower concentrations ($< 7 \mu\text{M}$) north of the Subantarctic Front (Table 1).

PO_4 followed a very similar pattern with concentrations generally greater than 1 μM south of the Subantarctic Front and $< 0.6 \mu\text{M}$ to the north. Silicic acid concentrations were divided by the PF, being generally less than 2 μM to the north and up to 78.5 μM to the south (Table 1). \bar{E}_{MLD} was highest on the Patagonian Shelf ($\sim 40 \text{ mol PAR m}^{-2} \text{ d}^{-1}$) and generally less than 10 $\text{mol PAR m}^{-2} \text{ d}^{-1}$ south of the Subantarctic Front (Table 1). There was no distinct latitudinal trend in pH or $p\text{CO}_2$. Surface water pH was generally greater than 8.06, ranging from 8.03 on the Kerguelen Plateau to 8.13 in the Subtropical Front southwest of Australia (Table 1). Surface water $p\text{CO}_2$ ranged from 299 to 444 μatm with both extremes in the vicinity of the Atlantic STF (Table 1). Chl *a* concentrations were variable across the oceanic gradients, highest on the Patagonian Shelf (2.78 mg m^{-3}), and on average less than 1 mg m^{-3} in the South Atlantic compared with less than 0.5 mg m^{-3} in the southern Indian Ocean (Table 1).

3.2 Coccolithophores and diatoms

The most frequently occurring and abundant size group within the coccolithophore and diatom counts were the nanoplankton (cells 2–20 μm). Large diatom species (cells $> 20 \mu\text{m}$) were found in higher numbers (up to 50 cells mL^{-1}) south of the PF. Consideration of community biomass would potentially reduce the dominance of the nanoplankton relative to microplankton in the GCB. However, converting from cell size to biomass is not straightforward for diatoms, as highlighted by Leblanc et al. (2012), and to avoid such issues we consider species abundance only. Total cell abundances were less than 1000 cells mL^{-1} at most stations (Table 2), which are indicative of late summer, non-bloom conditions. In the South Atlantic, the highest abundance of coccolithophores was on the Patagonian Shelf (station GCB1-16; 1636 cells mL^{-1}) and the highest abundance

Table 1. Details of Great Calcite Belt sampling stations including station and cruise identifier, date of sample collection (DD.MM.YYYY), station position decimal latitude (Lat) and longitude (Long), sea surface temperature (SST), surface salinity (Sal), mixed layer average irradiance (\bar{E}_{MLD}), surface macronutrient concentrations (nitrate and nitrite, NO_x ; phosphate, PO_4 ; silicate, $\text{Si}(\text{OH})_4$; ammonia, NH_4), and surface carbonate chemistry parameters (normalized total alkalinity, At; dissolved inorganic carbon, Ct; pH; partial pressure of carbon dioxide, $p\text{CO}_2$; calcite saturation state, Ω_{calcite} ; surface chlorophyll a , Chl a , measured in mg m^{-3}).

Station	Date	Lat ° S	Long ° E	SST ° C	Sal	\bar{E}_{MLD} molPAR $\text{m}^{-2}\text{d}^{-1}$	NO_x μM	PO_4 μM	$\text{Si}(\text{OH})_4$ μM	NH_4 μM	At $\mu\text{mol kg}^{-1}$	Ct $\mu\text{mol kg}^{-1}$	pH	$p\text{CO}_2$ μatm	Ω_{calcite}	Chl a mg m^{-3}
GCB1-6	14.01.2011	51.79	-56.11	8.6	34.0	17.8	14.2	1.05	1.7	0.64	2336	2138	8.09	367	3.3	0.84
GCB1-16	17.01.2011	46.26	-59.83	11.8	33.8	39.8	6.5	0.54	0.0	0.15	2333	2100	8.12	407	3.8	2.78
GCB1-25	20.01.2011	45.67	-48.95	16.1	35.1	25.5	0.0	0.23	0.2	0.16	2320	2047	8.12	390	4.6	0.73
GCB1-32	22.01.2011	40.95	-45.83	20.0	35.6	36.7	0.1	0.11	1.1	0.05	2307	2029	8.07	444	4.8	0.05
GCB1-46	26.01.2011	42.21	-41.21	18.3	34.9	16.0	0.2	0.19	0.3	0.00	2328	2050	8.09	356	4.7	0.09
GCB1-59	29.01.2011	51.36	-37.84	5.9	33.8	7.9	17.5	1.22	1.7	0.67	2368	2184	8.10	325	3.1	0.71
GCB1-70	01.02.2011	59.25	-33.15	1.1	34.0	9.7	22.3	1.74	78.5	1.54	2388	2235	8.10	407	2.6	0.13
GCB1-77	03.02.2011	57.28	-25.98	1.4	33.9	11.9	20.7	1.55	68.8	1.00	2386	2225	8.12	405	2.7	0.90
GCB1-85	05.02.2011	53.65	-17.75	4.1	33.9	8.9	19.1	1.33	0.7	0.30	2369	2191	8.12	363	3.0	1.11
GCB1-92	07.02.2011	50.40	-10.80	5.9	33.8	9.5	17.5	1.27	1.4	0.37	2362	2182	8.10	351	3.0	0.57
GCB1-101	09.02.2011	46.31	-3.21	11.0	34.0	17.1	12.5	0.95	0.6	0.16	2345	2134	8.08	400	3.5	0.46
GCB1-109	11.02.2011	42.63	3.34	15.1	34.4	20.0	5.3	0.56	0.8	0.00	2332	2098	8.07	359	4.0	0.39
GCB1-117	12.02.2011	39.00	9.49	18.8	35.0	19.4	0.0	0.20	0.7	0.06	2321	2047	8.08	299	4.7	0.32
GCB2-5	21.02.2012	37.09	39.48	21.0	35.5	11.2	0.0	0.05	1.1	0.07	2310	2005	8.10	340	5.2	0.12
GCB2-13	23.02.2012	40.36	43.50	18.4	35.3	13.7	0.1	0.17	0.2	0.02	2307	2032	8.09	351	4.7	0.19
GCB2-27	26.02.2012	45.82	51.05	7.7	33.7	5.8	20.1	1.35	2.9	0.14	2344	2194	8.00	425	2.6	0.47
GCB2-36	28.02.2012	46.74	57.48	8.1	33.7	8.7	18.9	1.40	1.7	0.49	2363	2175	8.08	355	3.1	0.21
GCB2-43	01.03.2012	47.52	64.04	6.5	33.7	5.9	21.7	1.53	0.5	0.38	2358	2197	8.04	387	2.8	0.34
GCB2-53	02.03.2012	49.30	71.32	5.1	33.7	8.5	23.8	1.66	7.1	0.17	2359	2210	8.03	396	2.6	0.41
GCB2-63	04.03.2012	54.40	74.56	3.5	33.8	3.0	25.3	1.70	10.5	0.21	2363	2210	8.07	360	2.6	0.26
GCB2-73	06.03.2012	59.71	77.75	1.1	33.9	4.3	28.0	1.91	40.4	0.34	2372	2233	8.07	360	2.4	0.29
GCB2-87	10.03.2012	54.25	88.14	3.4	33.9	4.3	24.2	1.69	9.0	0.45	2367	2216	8.06	367	2.6	0.28
GCB2-93	12.03.2012	49.81	94.13	7.8	34.0	5.9	17.5	1.27	1.5	0.26	2345	2149	8.10	333	3.3	0.18
GCB2-100	13.03.2012	44.62	100.50	13.0	34.8	4.7	6.4	0.55	0.2	0.15	2328	2083	8.11	326	4.1	0.33
GCB2-106	15.03.2012	40.13	105.38	17.0	35.4	12.8	0.1	0.14	0.3	0.03	2318	2029	8.13	313	4.9	0.24
GCB2-112	17.03.2012	40.26	109.60	15.8	34.9	11.1	3.6	0.43	0.2	0.00	2323	2060	8.11	332	4.4	0.36
GCB2-119	20.03.2012	42.08	113.40	13.8	34.8	11.2	5.3	0.55	0.2	0.01	2320	2080	8.10	342	4.1	0.27

Table 2. Whole cell abundances of coccolithophores and diatoms in surface samples of the Great Calcite Belt, the number of species in each group (S), Pielou's evenness (J' ; ***) indicates that J' was not calculated because only one species was present), the dominant species, and its percentage contribution to the total numerical abundance of coccolithophores (%Co) or diatoms (%D). The $^+$ symbol denotes where one species had almost total numerical dominance (> 99.8%), with only one or two cells of a separate species enumerated, and was therefore rounded up to 100%. Holococcolithophores are abbreviated as Holococco. "Position" denotes the location relative to the Southern Ocean fronts and zones (Z; north of the defined front) as defined by Orsi et al. (1995), and the letters after the front abbreviation denote specific locations and proximity to landmasses: Patagonian Shelf (PS), north of South Georgia (n SG), South Sandwich Islands (SS), Crozet Islands (Cr), Kerguelen Island (K), and Heard Island (H).

Station	Position	Coccolithophores (Co)				Diatoms (D)					
		Cell mL ⁻¹	S	J'	Dominant species	% of Co	Cell mL ⁻¹	S	J'	Dominant species	% of D
GCB1-6	SAF, PS	243	2	0.02	<i>E. huxleyi</i>	100 ⁺	127	15	0.79	<i>C. debilis</i>	26
GCB1-16	SAF, PS	1636	2	0.00	<i>E. huxleyi</i>	100 ⁺	4610	5	0.11	<i>F. pseudonana</i>	96
GCB1-25	SAFZ	55	9	0.67	<i>S. mollischi</i>	38	28	10	0.84	<i>Pseudo-nitzschia</i> spp.	37
GCB1-32	STF	23	8	0.83	<i>U. tenuis</i>	31	19	8	0.70	<i>Nitzschia</i> spp.	55
GCB1-46	STF	3	1	***	Holococco	100	4	3	0.91	<i>Chaetoceros</i> spp.	56
GCB1-59	sPF, n SG	565	1	***	<i>E. huxleyi</i>	100	183	30	0.72	<i>T. nitzschoides</i>	29
GCB1-70	sPF	103	1	***	<i>E. huxleyi</i>	100	720	24	0.29	<i>F. nana</i>	81
GCB1-77	sPF, SS	2	1	***	<i>E. huxleyi</i>	100	6893	18	0.04	<i>F. nana</i>	98
GCB1-85	sPF	28	1	***	<i>E. huxleyi</i>	100	151	30	0.77	<i>C. aequatorialis</i> sp.	22
GCB1-92	PFZ	77	2	0.13	<i>E. huxleyi</i>	98	111	28	0.73	<i>Pseudo-nitzschia</i> spp.	32
GCB1-101	SAFZ	92	7	0.57	<i>E. huxleyi</i>	68	52	11	0.57	<i>F. pseudonana</i>	59
GCB1-109	SAFZ	39	9	0.90	<i>E. huxleyi</i>	25	129	17	0.55	<i>Pseudo-nitzschia</i> spp.	61
GCB1-117	STF	15	6	0.88	<i>U. tenuis</i>	35	209	9	0.13	<i>C. closterium</i>	95
GCB2-5	STFZ	37	15	0.69	<i>E. huxleyi</i>	46	6	8	0.76	<i>Nanoneis hasleae</i>	47
GCB2-13	STFZ	51	17	0.61	<i>E. huxleyi</i>	57	28	7	0.57	<i>Nitzschia</i> spp. < 20 µm	67
GCB2-27	SAF, Cr	478	6	0.04	<i>E. huxleyi</i>	99	375	24	0.28	<i>F. pseudonana</i>	83
GCB2-36	SAF	166	8	0.32	<i>E. huxleyi</i>	83	155	32	0.69	<i>F. pseudonana</i>	33
GCB2-43	PFZ	12	4	0.18	<i>E. huxleyi</i>	95	90	25	0.57	<i>F. pseudonana</i>	54
GCB2-53	sPF, K	51	3	0.90	<i>E. huxleyi</i>	56	512	28	0.39	<i>F. pseudonana</i>	47
GCB2-63	sPF, H	132	1	***	<i>E. huxleyi</i>	100	254	24	0.38	<i>F. pseudonana</i>	71
GCB2-73	sPF	0	0	***	n/a	n/a	538	24	0.55	<i>F. pseudonana</i>	56
GCB2-87	sPF	106	1	***	<i>E. huxleyi</i>	100	184	29	0.55	<i>F. pseudonana</i>	42
GCB2-93	PFZ	100	11	0.33	<i>E. huxleyi</i>	80	75	29	0.67	<i>Pseudo-nitzschia</i> spp.	37
GCB2-100	SAFZ	123	13	0.26	<i>E. huxleyi</i>	86	164	26	0.44	<i>Pseudo-nitzschia</i> spp.	67
GCB2-106	STF	90	19	0.77	<i>E. huxleyi</i>	29	80	22	0.58	<i>Pseudo-nitzschia</i> spp.	54
GCB2-112	STF	123	12	0.35	<i>E. huxleyi</i>	80	257	27	0.38	<i>Pseudo-nitzschia</i> spp.	74
GCB2-119	SAFZ	121	17	0.32	<i>E. huxleyi</i>	82	68	21	0.55	<i>Pseudo-nitzschia</i> spp.	47

of diatoms was east of the South Sandwich Islands (station GCB1-77; 6893 cells mL⁻¹; Table 2). In the southern Indian Ocean, coccolithophore abundance was highest near the Crozet Islands (station GCB2-27; 472 cells mL⁻¹), and diatom abundance was highest at the most southerly station (station GCB2-73; 538 cells mL⁻¹; Table 2). There were no stations in the southern Indian Ocean where coccolithophore and diatom abundances were greater than 1000 cells mL⁻¹ (Fig. 2, Table 2). Additionally, the silicifying chrysophyte *Tetraparma* sp. was particularly abundant east of the South Sandwich Islands (station GCB1-77) at a cell density of 2000 cells mL⁻¹, though they were present in low numbers (< 5 cells mL⁻¹) at three more stations in the South Atlantic and absent throughout the rest of the GCB.

Coccolithophores dominated the biomineralizing community at 12 stations in terms of abundance north of the PF (Fig. 2, Table 2). On average coccolithophores contributed approximately 38 % to total (coccolithophore and diatom) abundance in the GCB. Coccolithophores were greater than 75 % of the total abundance at only one station to the north of South Georgia (station GCB1-59) and never accounted for 100 % of total cell numbers. Twenty-eight species of coccolithophores were identified as intact coccospheres across the GCB. Coccolithophore diversity decreased south towards 60° S, with the highest coccolithophore diversity (19 species) found in the vicinity of the STF in the eastern part of the southern Indian Ocean (station GCB2-106), while coccolithophore abundance was more evenly distributed between the different species in the lower latitudes (i.e., high J' ; Table 2). *Emiliania huxleyi* was the most numerically abundant coccolithophore at all but four stations and was encountered in the mixed layer at all stations except one (station GCB2-73, the most southerly station in the Indian Ocean). Other coccolithophore species (e.g., *Syracosphaera* spp. and *Umbellosphaera* spp.) were present north of the PF throughout the GCB and were most abundant north of the STF. At stations south of the SAF (50° S) only one (*E. huxleyi*) or two species (*E. huxleyi* and *Pappamonas* sp.) were observed as intact coccospheres.

Diatoms dominated 15 stations in terms of biomineralizing plankton abundance across all environments sampled (Fig. 2, Table 2), being found in every sample analyzed and contributing 62 % (on average) to total (coccolithophores + diatoms) abundance. Diatoms made up 100 % of the total cell counts at the most southerly station in the southern Indian Ocean (station GCB2-73) and 99.7 % east of the South Sandwich Islands (station GCB1-77; Fig. 2). Seventy-six species of diatom were identified as intact cells across the entire GCB. The most frequently occurring species in the GCB were small (< 5 µm in length) *Fragilariopsis* spp. The highest abundance of diatoms in the South Atlantic Ocean (6893 cells mL⁻¹) was dominated by *F. nana* east of the South Sandwich Islands (station GCB1-77). The highest diatom abundance in the southern Indian Ocean (538 cells mL⁻¹) was dominated by *F. pseudonana* at the

most southerly station (station GCB2-73) sampled. Another frequently dominant diatom was *Pseudo-nitzschia* spp., which was most abundant north of the PF (Table 2).

Diatom species richness increased south towards 60° S with the contribution of the different diatom species to the total biomineralizing plankton abundance fairly even ($J' > 0.5$, Table 2), except at stations (stations GCB1-70, GCB1-77, GCB2-27, and GCB2-63) where *Fragilariopsis* spp. < 5 µm were dominant (> 70 % of the diatom population, $J' < 0.5$). The highest diatom species richness (32 species) was found in the GCB south of the SAF (station GCB2-36) at a temperature of 8 °C, in HNLSiLC conditions (NO_x 18.9 µM, silicic acid 1.7 µM, 0.21 mg Chl *a* m⁻³).

3.3 Statistical analysis

Three of the environmental variables were removed from the statistical analysis following a Spearman's rank (r_s) correlation analysis (Table S1 in the Supplement). NO_x and PO₄ had a strong significant positive correlation ($r_s = 0.961$, $p < 0.0001$), so NO_x was deemed representative of the distribution of both nutrients. Sea surface temperature displayed significant negative correlations with both C_T ($r_s = -0.981$, $p < 0.0001$) and A_T ($r_s = -0.953$, $p < 0.0001$), so sea surface temperature was taken as being representative of these two variables of the carbonate chemistry system.

The variation in environmental variables across the GCB was examined using a principal component analysis (PCA), which simplifies environmental variability by combining closely correlated variables into principal components in order to account for the greatest variance in the data with the fewest components. The first principal component (PC1) accounted for 58 % of the variation in environmental variables, with an additional 17 % of environmental variation described by PC2 (Table 3). PC1 describes the main latitudinal gradients of environmental changes across the GCB (decreasing SST, increasing macronutrients). PC1 is a predominantly linear combination of SST, salinity, NO_x, silicic acid, NH₄, and Ω_{calcite}; there is a significant positive correlation of PC1 with SST and salinity and a significant negative correlation with all other variables (Table 3). PC2 represented the environmental variation in the GCB occurring independently of latitude and was driven predominantly by variation in $p\text{CO}_2$, with weaker influences from \bar{E}_{MLD} and pH (Table 3). PC2 had significant positive correlations with $p\text{CO}_2$ and \bar{E}_{MLD} and a negative correlation with pH.

The SIMPROF routine identified the stations in the GCB that had statistically similar coccolithophore and diatom community composition through a comparison of Bray–Curtis similarities. Six statistically significant groups ($p < 0.05$) were defined across the GCB (Fig. 3). Three of these groups (A, B, C) were specific to the South Atlantic Ocean (Fig. 3). For example, groups A and B represented individual stations GCB1-46 and GCB1-117, respectively, in the subtropical region of the South Atlantic Ocean. The

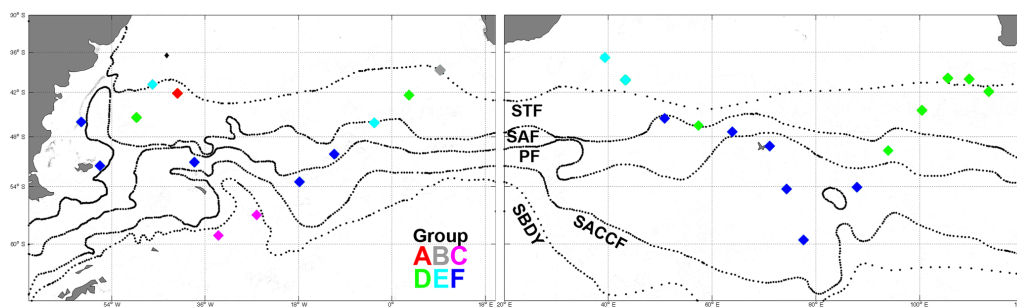


Figure 3. Statistically significant groups of coccolithophore and diatom communities in the Great Calcite Belt as identified by the SIMPROF routine. The colors designate which statistical group defines the coccolithophore and diatom assemblage at each station as shown in the group key. Fronts are defined as in Fig. 1. See Table 4 for full group species descriptions.

Table 3. Principal component (PC) scores, percentage of variation described (%V), and the Pearson's product moment correlation associated with each variable and its significance level: $p < 0.0001$ ***, $p < 0.001$ ***, $p < 0.005$ *, $p < 0.01$, $p < 0.05$.

Variable	PC1 – EV 5 (58 %)	PC2 – EV 1.5 (17 %)		
Temp	0.42	(0.97***)	0.08	(−0.10)
Salinity	0.36	(0.90***)	0	–
\bar{E}_{MLD}	0.24	(−0.55*)	0.5	(0.62**)
NO_x	−0.4	(−0.91***)	−0.05	(−0.06)
$Si(OH)_4$	−0.35	(−0.77***)	0.02	(−0.03)
NH_4	−0.35	(−0.81***)	−0.07	(−0.09)
pH	0.18	(−0.39)	−0.42	(−0.50*)
pCO_2	−0.15	(−0.33)	0.75	(0.89***)
$\Omega_{calcite}$	0.43	(−0.99***)	−0.02	(−0.02)

most southerly stations in the South Atlantic Ocean (stations GCB1-70 and GCB1-77) defined group C (Fig. 3). Groups D, E, and F included stations across the GCB in both ocean regions. Here, group D was defined by eight stations sampled predominantly north of the SAF, while group F was defined by 11 stations predominantly sampled south of the SAF (Fig. 3). These statistically defined similar community structures indicate that although the GCB covers a wide expanse of ocean, the community structure is consistently latitudinally defined across its longitudinal range.

A SIMPER routine statistically identified the species that define the difference between (and the similarity within) the statistically different community structures defined by the SIMPROF routine (Table 4). The abundance and distribution of four phytoplankton species (*E. huxleyi*, *Pseudo-nitzschia* spp., *F. nana*, and *F. pseudonana*; Fig. 4) were identified as having the most significant contribution to differences in community structure across the GCB (Table 4). *Emiliania huxleyi* and *F. pseudonana* were the most numerically dominant coccolithophore and diatom species, respectively, across the GCB (Table 2). *Fragilariopsis pseudonana* was the numerically dominant diatom (> 30 %) at seven stations in the southern Indian Ocean (Table 2). The diatom with the high-

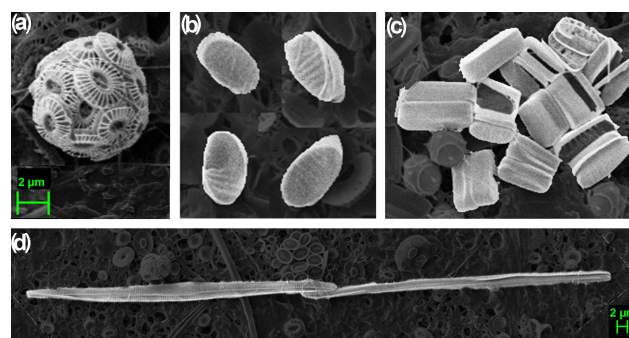


Figure 4. SEM images of the four phytoplankton species identified by the SIMPER analysis as characterizing the significantly different community structures: (a) *E. huxleyi*, (b) *F. pseudonana*, (c) *F. nana*, and (d) *Pseudo-nitzschia* spp.

est abundance, *F. nana* ($6797 \text{ cells mL}^{-1}$), was almost exclusively found in the South Atlantic Ocean (Table 2) and the more frequently occurring *Pseudo-nitzschia* spp. was present at all but one station.

The nonmetric multidimensional scaling (nMDS) plot of the Bray–Curtis similarities (Fig. 5) shows the station distribution with respect to the SIMPROF-defined groups (Fig. 5a), the four main species (Fig. 5b–e), and also holococcolithophores (Fig. 5f). The more closely clustered the stations, the more similar their biomineralizing species composition. Groups A and B were defined by the absence of *E. huxleyi* (Fig. 5b) and the presence of either holococcolithophores (group A; Fig. 5f) or the diatom *Cylindrotheca* sp. (group B). Group C was defined by the dominance of *F. nana* (Table 4; Fig. 5d) and low contributions from *E. huxleyi* and *Pseudo-nitzschia* spp. (Table 2; Fig. 5b, e), resulting in a significant difference from the other groups. Group D had high total species diversity overall (19–41 species; Table 2) and was defined by similar relative abundances of *E. huxleyi* and *Pseudo-nitzschia* spp., which were not found elsewhere (Fig. 5b, e). Group E, composed of stations north of the SAF (Figs. 3, 5a), included *E. huxleyi*, *U. tenuis*, and holococcolithophores (Table 4, Fig. 5b, f). The low abundance and

Table 4. Phytoplankton assemblage groups identified using the SIMPROF routine at $p < 0.05$ in the GCB (see also Fig. 3) from the South Atlantic (GCB1) and the southern Indian (GCB2) oceans. Location is indicated as in Fig. 2. Group average similarity (Group Av.Sim%) defines the percentage of similarity of the community structure in all the stations within each group. The defining species contributing $> 50\%$ to the species similarity for each group as identified through the SIMPER routine are presented alongside the average similarity for each species in each group (Average similarity); higher “Similarity SD” indicates more consistent contribution to similarity within the group. The percentage of contribution per species to the group similarity (Contribution%) was also calculated. Group averages not calculable (n/a) for single station groups A and B.

Group	Station	Location	Group Av.Sim%	Defining species	Average similarity	Similarity SD	Contribution%	
A	GCB1-46	STF	n/a	Holococco	n/a	n/a	n/a	
B	GCB1-117	STF	n/a	<i>Cylindrotheca</i> sp.	n/a	n/a	n/a	
C	GCB1-70 GCB1-77	SBDY	54.5	<i>F. nana</i>	53.3	n/a	97.8	
D	GCB1-25	N of PF	47.6	<i>E. huxleyi</i>	13.9	2.68	29.3	
	GCB1-109			<i>Pseudo-nitzschia</i> spp.	12.7	3.6	26.7	
	GCB2-36							
	GCB2-93							
	GCB2-100							
	GCB2-106							
	GCB2-112 GCB2-119							
E	GCB1-32	N of SAF	42.3	<i>E. huxleyi</i>	18.9	3.8	44.8	
	GCB1-101			Holococco	8.45	4.01	20	
	GCB2-5							
	GCB2-13							
F	GCB1-6	PS	40.6	<i>E. huxleyi</i>	15.1	1.51	37.3	
	GCB1-16	S of SAF		<i>F. pseudonana</i>	14.2	1.25	35	
	GCB1-59							
	GCB1-85							
	GCB1-92							
	GCB2-27							
	GCB2-43							
	GCB2-53							
	GCB2-63							
	GCB2-73							
	GCB2-87							

diversity ($3\text{--}125\text{ cells mL}^{-1}$, 7–11 species; Table 2) of diatoms within group E separated it from the other groups. The combination of *E. huxleyi*, *F. pseudonana*, and *Pseudo-nitzschia* spp. that defined group F (Table 4, Fig. 5b, c, e) represented stations on the Patagonian Shelf and south of the SAF (Figs. 3, 5a). The almost monospecific *E. huxleyi* coccolithophore community (Table 2) in group F highlights its strong dissimilarity from the other community structure groups identified (Fig. 5).

The influence of environmental variables on the biogeography of coccolithophores and diatoms in the GCB was assessed using the BEST routine. The strongest Spearman’s rank correlation ($r_s = 0.55$, $p < 0.001$) between all possible environmental variables and the biogeographical patterns observed came from a combination of five vari-

ables: (1) SST, (2–4) macronutrients (NO_x , silicic acid, NH_4), and (5) $p\text{CO}_2$. This was followed by a correlation of $r_s = 0.54$ ($p < 0.001$) that included these parameters and Ω_{calcite} . Salinity was included in the third-highest correlation, whereas \bar{E}_{MLD} and pH did not rank as significant factors in the BEST analysis.

4 Discussion

4.1 Biogeography of coccolithophores and diatoms in the Great Calcite Belt

Studies of Southern Ocean phytoplankton productivity have generally focused on the microphytoplankton (Barber and Hiscock, 2006) as these species contribute around 40 % to to-

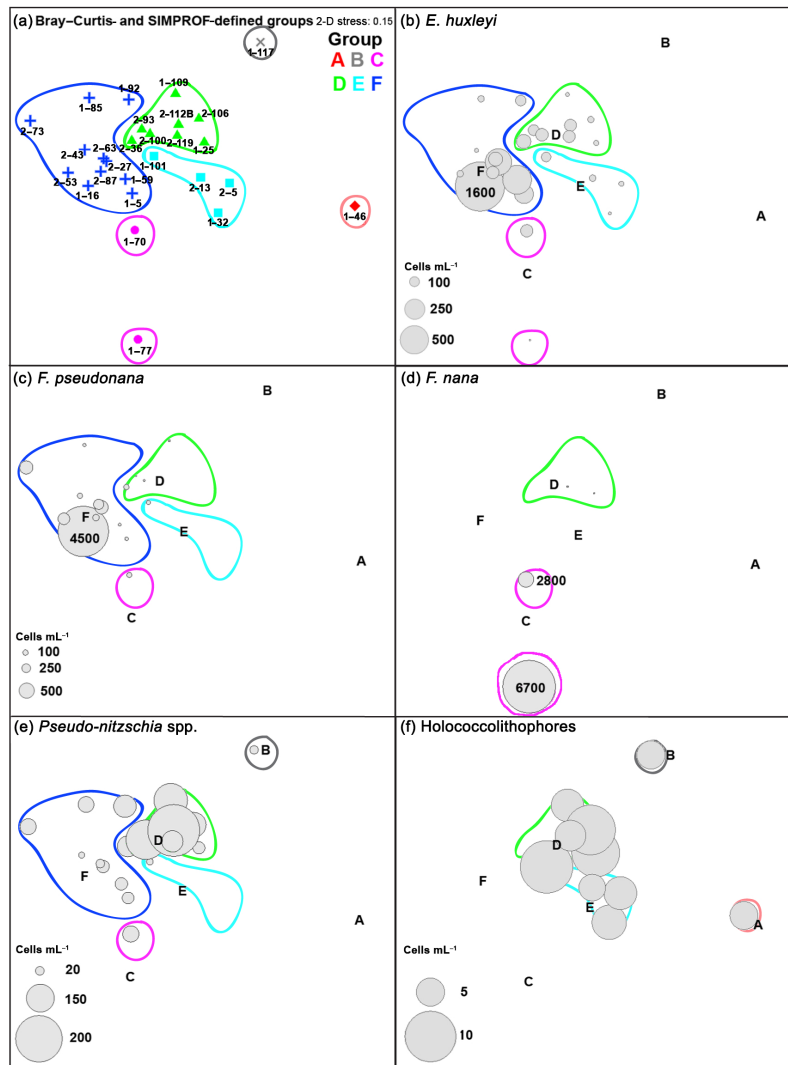


Figure 5. Two-dimensional nonmetric multidimensional scaling (nMDS) ordination of station groupings (a) as defined by the SIMPROF routine, with group color identifiers as in Fig. 3; relative distances between samples represent the similarity of species composition between phytoplankton communities. Stations with statistically similar species composition are clustered together, whereas stations with low statistical similarity in terms of species composition are more widely spaced. Overlay of bubble plots of the defining species abundance (cells mL⁻¹) characterizing the statistically significant groups in the GCB (see also Table 4): (b) *E. huxleyi* abundance, (c) *F. pseudonana* abundance, (d) *F. nana* abundance, (e) *Pseudo-nitzschia* spp. abundance, and (f) Holococcolithophores abundance. The two-dimensional stress of 0.15 gives a “reasonable” representation of the data in a 2-D space (Clarke and Warwick, 2001).

tal oceanic primary production (Sarthou et al., 2005; Uitz et al., 2010). However, nanoplankton and picoplankton are becoming increasingly recognized as important contributors to total phytoplankton biomass, productivity, and export in the Southern Ocean (e.g., Boyd, 2002; Froneman et al., 2004; Uitz et al., 2010; Hinz et al., 2012), as the dominant size group in both post-bloom (Le Moigne et al., 2013) and non-bloom conditions (Barber and Hiscock, 2006).

In this study, coccolithophores were generally numerically dominant at stations sampled north of the PF, particularly around the Subantarctic Front, whereas diatoms were dominant at stations south of the PF (Fig. 2). There was also a sig-

nificantly different species distribution (a priori ANOSIM; $R = 0.227$, $p < 0.01$) north and south of the Subantarctic Front, which has been previously identified as the divider between calcite- and opal-dominated export in the Southern Ocean (e.g., Honjo et al., 2000; Balch et al., 2016). Diatoms were more abundant (~ 570 cells mL⁻¹) than coccolithophores (~ 160 cells mL⁻¹) on average in the entire GCB. This is in contrast to Eynaud et al. (1999) for the South Atlantic Ocean at a similar time of year, who reported a peak in coccolithophore cell abundance in the vicinity of the PF (a feature that was not observed in this study). These differences are likely due to the variability of Southern Ocean

plankton on short temporal scales (Mohan et al., 2008), including variability in the seasonal progression of the spring bloom (Bathmann et al., 1997).

The coccolithophore *E. huxleyi* and diatoms *F. pseudonana*, *F. nana*, and *Pseudo-nitzschia* spp. (Fig. 4) were all identified as being central to defining the statistical similarities within, and the differences between, the different biomineralizing phytoplankton groups (Table 4, Fig. 5). Three of these species (*E. huxleyi*, *F. nana*, and *F. pseudonana*) are part of the nanoplankton, whilst *Pseudo-nitzschia* spp. is at the lower end of the size range of the microplankton (*Pseudo-nitzschia* spp. is $> 20 \mu\text{m}$ in length but $< 5 \mu\text{m}$ in width) and contributes significantly to biomass in Southern Ocean HNLC regions (Boyd, 2002). *Emiliania huxleyi* and *Fragilariopsis* spp. smaller than $10 \mu\text{m}$ have been identified as two of the most abundant biomineralizing phytoplankton further south in the Scotia Sea (Hinz et al., 2012). Our results further highlight that nanoplankton have the potential to contribute a significant proportion to GCB community composition alongside the larger phytoplankton (including large diatoms) typical of HNLC regions.

Abundances of HNLC diatoms, such as *F. kerguelensis* ($< 10 \text{ cells mL}^{-1}$), *T. nitzschioides* ($< 20 \text{ cells mL}^{-1}$), and large *Chaetoceros* spp. ($< 10 \text{ cells mL}^{-1}$), were lower than those observed in other studies (e.g., Poulton et al., 2007; Armand et al., 2008; Korb et al., 2010, 2012). Furthermore, the absence of the diatom *Eucampia antarctica* ($< 1 \text{ cell mL}^{-1}$) in this study does not reflect the typical assemblage (sometimes $> 600 \text{ cells mL}^{-1}$) found in previous studies (e.g., Kopczynska et al., 1998; Eynaud et al., 1999; de Baar et al., 2005; Poulton et al., 2007; Salter et al., 2007; Korb et al., 2010). Low abundances of the large-celled diatoms in the silicic-acid-replete regions may partly relate to the small filter area analyzed using SEM; in this study the area imaged equates to a relatively small volume of water (2–6 mL depending on magnification) relative to the larger volumes (10–50 mL) often examined for light microscopy in other studies. Large, rare cells may not be enumerated from such small sample volumes; however, the numerically abundant nanoplankton groups were well represented in SEM images. Conversely, samples preserved in acidic Lugol's solution for light microscopy analysis are biased towards larger species since small diatoms ($< 10 \mu\text{m}$) are not clearly visible and coccolithophores are not well preserved (Hinz et al., 2012). In the future, a combination of both imaging techniques is recommended to fully express the phytoplankton community structure of the Southern Ocean.

4.2 *Emiliania huxleyi* in the Great Calcite Belt

The importance of coccolithophores in the GCB was examined via species composition and the abundance of intact cells, focusing on areas identified as having high PIC reflectance from underway sampling and satellite observations (Balch et al., 2014, 2016; Hopkins et al., 2015). Higher

species diversity of coccolithophores occurred north of the STF (i.e., 6–19 species; Table 2). Coccolithophores are diverse in the stratified and low-nutrient waters associated with lower latitudes (Winter et al., 1994; Poulton et al., 2017). Only a few species are found in the colder waters south of the STF (Mohan et al., 2008), the most successful being *E. huxleyi*, which was observed at an abundance of $103 \text{ cells mL}^{-1}$ at 1°C in this study in the South Atlantic (station GCB1-70). The 2°C isotherm has been previously assumed to represent the southern boundary of *E. huxleyi* (e.g., Verbeek, 1989; Mohan et al., 2008), and interannual variability could be influenced by the movement of the southern front of the Antarctic Circumpolar Current (Holligan et al., 2010). The Southern Ocean *E. huxleyi* morphotype (Cook et al., 2011; Poulton et al., 2011) may therefore have a wider temperature tolerance than its Northern Hemisphere equivalent (Hinz et al., 2012) and has been observed poleward of 60°S further east in the Southern Ocean (Cubillos et al., 2007) and across the Drake Passage (Charalampopoulou et al., 2016). There were three distinct *E. huxleyi* occurrences (the Patagonian Shelf, north of South Georgia, and north of the Crozet Islands) within the GCB where *E. huxleyi* contributed $> 50\%$ of the total cell counts of biomineralizing phytoplankton. *Emiliania huxleyi* was most abundant ($1636 \text{ cells mL}^{-1}$) on the Patagonian Shelf and was the most frequently occurring coccolithophore across the entire GCB. The main *E. huxleyi* occurrences are further discussed below to examine why this species is so widely distributed in the GCB.

4.2.1 Patagonian Shelf

The Patagonian Shelf is a well-known region for *E. huxleyi* blooms, as observed in satellite imagery between November and January (Signorini et al., 2006; Painter et al., 2010; Balch et al., 2011, 2014; Garcia et al., 2011). The *E. huxleyi* cell abundance observed in this study ($\sim 1600 \text{ cells mL}^{-1}$) was similar to that found by Poulton et al. (2013; $> 1000 \text{ cells mL}^{-1}$). Using a value of $0.2 \text{ pg Chl } a \text{ cell}^{-1}$ (Haxo, 1985) and following the approach in Poulton et al. (2013), such *E. huxleyi* abundance levels are equivalent to estimated contributions of only $\sim 12\%$ to the total Chl *a* signal ($\sim 2.8 \text{ mg m}^{-3}$). This estimate is similar to that estimated in an identical way by Poulton et al. (2013) and highlights the significant contribution of phytoplankton other than coccolithophores (flagellates, diatoms) to phytoplankton biomass and production during coccolithophore blooms. It should be noted that the cell Chl *a* content from Haxo (1985) falls at the lower end of the current range of measurements for *E. huxleyi* cell Chl *a* content (e.g., $0.24\text{--}0.38 \text{ pg Chl } a \text{ cell}^{-1}$; Daniels et al., 2014) and leads to conservative estimates of Chl *a* contribution from this species. These data, combined with satellite observations, support the hypothesis of a repeating phytoplankton structure on an interannual basis, although the contribution of *E. huxleyi* to primary production may vary. The optimum range for *E. huxleyi*

blooms on the Patagonian Shelf has been identified as between 5 and 15 °C at depleted silicic acid levels relative to nitrate (Balch et al., 2014, 2016). During this study, silicic acid was at almost undetectable levels on the Patagonian Shelf (Table 1), with the source water for this region being Southern Ocean HNLSiLC waters transported northwards via the Falklands current (Painter et al., 2010; Poulton et al., 2013). The persistently low silicic acid availability and residual nitrate (defined as $[\text{NO}_3^-] - [\text{Si}(\text{OH})_4]$) on the Patagonian Shelf is therefore an ideal environment for *E. huxleyi* to outgrow large, fast-growing diatoms (Balch et al., 2014).

4.2.2 South Georgia

South Georgia is renowned for intense diatom blooms of over 600 cells mL⁻¹ with Chl *a* over 10 mg m⁻³ and integrated primary production up to 2 g C m⁻² d⁻¹ (Korb et al., 2008). However, *E. huxleyi* was the dominant species (> 75 % of total cell numbers) within the diatom and coccolithophore population at the station north of South Georgia (Table 2, Fig. 2). The associated calcite feature can also be identified from the satellite composite in Fig. 1 (38° E, 51° S). *Emiliania huxleyi* contributed approximately 15 %, calculated by applying a value of 0.2 pg Chl *a* cell⁻¹ (Haxo, 1985) following Poulton et al. (2013), to the total Chl *a* signal (0.71 mg m⁻³) around South Georgia. The high calcite feature at South Georgia was found at an SST of 5.9 °C, which is below the considered “optimum” growth conditions for *E. huxleyi* previously cultured (Paasche, 2001). This population of *E. huxleyi* was most likely an adapted cold-water morphotype (Cook et al., 2011, 2013; Poulton et al., 2011). The dominant diatom species here were *Actinocyclus* sp. and highly silicified *Thalassionema nitzschioides* with silicic acid concentrations likely limiting (1.7 μmol Si L⁻¹; Paasche 1973a, b), whereas NO_x concentrations (17.5 μmol N L⁻¹) and PO₄ concentrations (1.22 μmol P L⁻¹) can be considered replete. The low silicate concentrations could explain why *Eucampia antarctica* was not observed in this study, though it has been observed north of South Georgia (Korb et al., 2010, 2012). This indicates that preceding diatom growth depleted silicic acid (and other nutrients such as dissolved iron), allowing *E. huxleyi* to become more dominant in the population with a similar residual nitrate environment as found on the Patagonian Shelf (this study; Balch et al., 2014, 2016) and also in the North Atlantic (Leblanc et al., 2009).

4.2.3 Crozet Islands

The *E. huxleyi* feature north of the Crozet Islands with an abundance of 472 cells mL⁻¹ (the highest in the southern Indian Ocean) confirms the presence of coccolithophores in this region. Coccolithophore abundances have not previously been reported in this region, although elevated PIC had been observed and attributed to *E. huxleyi* (Read et al., 2007; Salter et al., 2007). Chl *a* was lowest (0.47 mg m⁻³)

at Crozet out of all three high PIC features, with *E. huxleyi* contributing ~ 20 % of this signal, calculated by applying a value of 0.2 pg Chl *a* cell⁻¹ (Haxo, 1985) following Poulton et al. (2013), which is proportionally higher than on the Patagonian Shelf and near South Georgia. Previous studies around the Crozet Islands and plateau (2004–2005) have found evidence of coccolithophores in sediment trap samples (Salter et al., 2007) and large (> 30 mmol C m⁻² d⁻¹) calcite fluxes (Le Moigne et al., 2012), though surface cell counts were unavailable (Read et al., 2007). The satellite-derived calcite signal was observed to increase after the main Chl *a* event in this study (Fig. S1 in the Supplement) and in previous years (Salter et al., 2007). An increase in coccolithophore abundance following a diatom bloom is also observed in similar oceanic regions from satellite-derived products (Hopkins et al., 2015) and is associated with depletion of dissolved iron and/or silicic acid (Holligan et al., 2010) in addition to a stable water column and increased irradiance (Balch et al., 2014).

4.2.4 Summary of biogeochemical characterization of coccolithophore occurrence and abundance

The Southern Ocean has been considered to have a biomineralizing phytoplankton community dominated by diatoms. This study highlights the fact that *E. huxleyi* can form distinct features within the GCB and contribute up to 20 % towards total Chl *a* in these features compared to an average of less than 5 % of Chl *a* across the rest of the GCB. Hence, *Emiliania huxleyi* is likely to have a more important role in the biogeochemical processes in the GCB than previously thought. This is particularly important to consider when assessing the impact on calcium-carbonate-associated export (e.g., Honjo et al., 2000; Balch et al., 2010, 2016) in the Southern Ocean. If *E. huxleyi* is migrating poleward with time (Winter et al., 2013), then the dynamics of the carbon system in the GCB may change, particularly south of the SAF where silicic-acid-derived export has historically been dominant (Honjo et al., 2000; Pondaven et al., 2000). Thus, it is essential to gain an understanding of the environmental factors driving the distribution of *E. huxleyi* (Winter et al., 2013; Charalampopoulou et al., 2016) amongst other phytoplankton in the GCB to better understand the biogeochemistry of the Southern Ocean.

4.3 Environmental controls on biogeography

The environmental variables that best describe coccolithophore and diatom species distribution in this study were SST, macronutrients (NO_x, silicic acid, NH₄), and *p*CO₂ (Spearman's rank correlation = 0.55, *p* < 0.001), with the second-highest correlation (Spearman's rank correlation = 0.54, *p* < 0.001) including the calcite saturation state (Ω_{calcite}). The inclusion of *p*CO₂ and Ω_{calcite} as important factors indicates a potential influence of carbonate chemistry on coccolithophore and diatom distribution (and vice versa)

in the GCB. However, Ω_{calcite} had a very strong positive correlation ($r = 0.964$, $p < 0.0001$) with SST (Table S1), and therefore separating the influences of the two variables was impossible in this study due to the tight coupling between carbonate chemistry and temperature (as also observed by Charalampopoulou et al., 2016).

4.3.1 Temperature

Temperature is recognized as a strong driving factor behind plankton biogeography and community composition (Raven and Geider, 1988; Boyd et al., 2010). The abundance of two of the dominant species, *E. huxleyi* and *F. pseudonana*, did not significantly correlate (Pearson's product moment correlation = 0.147, $p = 0.493$ and $r = -0.247$, $p = 0.357$ respectively) with SST, which does not agree with previous work (e.g., Mohan et al., 2008) and implies that *E. huxleyi* distribution is not solely determined by latitudinal variations in temperature. Nanoplankton are subject to high grazing pressure (Schmoker et al., 2013), with the growth and mortality of a species both directly influencing cell abundances (Poulton et al., 2010), which could result in nanoplankton patchiness in addition to the influence of temperature and/or other environmental gradients. In contrast, the negative correlation of *F. nana* (Pearson's product moment correlation = -0.976 , $p < 0.05$, $n = 4$) versus the positive correlation of *Pseudo-nitzschia* spp. (Pearson's product moment correlation = 0.544, $p < 0.05$, $n = 19$) with SST indicates that these two species have distinctly different physiological tolerances. Southern Ocean diatoms are often observed to have negative relationships with temperature (e.g., Eynaud et al., 1999; Boyd, 2002). *Pseudo-nitzschia* spp. was predominantly found in waters north of the PF in this study, as seen by Kopczynska et al. (1986), and is likely to be out-competed by other diatom species (e.g., *Chaetoceros* spp. and *Dactyliosolen* spp.) further south due to different nutrient affinities and requirements (Kopczynska et al., 1986), particularly for dissolved iron and silicic acid.

4.3.2 Nutrients

Macronutrient gradients, particularly silicic acid, are considered one of the key driving factors between the differences in community structure in the Southern Ocean (Nelson and Tréguer, 1992). NO_x (and PO_4 by association) was identified in the BEST test as an important factor in the variability of biomineralizing species distribution, but it did not significantly correlate with the four statistically dominant species (Fig. 4) contributing over 50 % to changes in species composition in the GCB.

Nitrate drawdown by Southern Ocean diatoms is limited by dissolved iron (dFe) availability south of the STF (Sedwick et al., 2002), which may explain the dominance of the nanoplankton (with lower dFe and macronutrient requirements; Ho et al., 2003) in this study as they are not affected

by low dFe concentrations as severely as the microplankton. The low silicic acid concentrations in the region between the SAF and the PF indicate that there was sufficient dFe to allow silicification and diatom growth, but either one or both of the macronutrients were then depleted to limiting concentrations (Assmy et al., 2013). As an essential nutrient for diatoms, silicic acid concentrations less than $2 \mu\text{M}$ were most common in the GCB, a level which is considered limiting for most diatom species (Paasche, 1973a, b; Egge and Asknes, 1992). However, even at stations with greater than $5 \mu\text{M}$ of silicic acid, the small diatom species ($< 10 \mu\text{m}$) were still dominant and represented over 40 % of the total coccolithophore and diatom assemblage (numerically). A significant positive correlation occurred between silicic acid and the small ($< 5 \mu\text{m}$) diatom *F. nana* (Pearson's product moment correlation = 0.986, $p < 0.05$, $n = 4$). *Fragilariopsis nana* may have a low cellular silicate requirement similar to *F. pseudonana* (Poulton et al., 2013) and relative to larger diatom species, so the high abundance of *F. nana* in the high-silicic-acid waters could be indicative of a seasonal progression driven by light and/or temperature rather than silicic acid dependence. *Fragilariopsis* spp. have been observed at high abundances near the Ross Sea ice shelf (Grigorov and Rigual-Hernandez, 2014), and high abundances of large diatoms in silicic-acid-replete (and dFe-replete) waters may occur further south than we sampled. In the South Atlantic and the South Pacific Ocean, silicic acid depletion moves southwards as spring to summer progresses, with maximum diatom biomass observed in late January at 65°S (Sigmon et al., 2002; Le Moigne et al., 2013).

A significant negative correlation between *E. huxleyi* and silicic acid (Pearson's product moment correlation = -0.410 , $p < 0.05$, $n = 24$) in this study has also been identified in the Scotia Sea (Hinz et al., 2012) and the Patagonian Shelf (Balch et al., 2014) in the Southern Ocean, as well as in the North Atlantic (Leblanc et al., 2009). Low silicic acid may be considered a positive selection pressure for coccolithophores (Holligan et al., 2010), especially when other macronutrients (and dFe) are replete. However, a few non-blooming coccolithophore species are now recognized as having silicic acid requirements, though this requirement is absent in *E. huxleyi* (Durak et al., 2016). Therefore, low silicic acid in the surface waters of the GCB may negatively impact coccolithophore species that have a silicic acid requirement, such as *Calcidiscus leptoporus*, and favor bloom-forming species that have no silicic acid requirement (e.g., *E. huxleyi*). To the south of the PF, silicic acid increased (from < 1 to $> 3 \mu\text{M}$) with five stations between the SAF and PF (and one south of the PF, station GCB1-59) all numerically dominated by *E. huxleyi*, while other stations to the south of the PF were dominated by diatoms (Fig. 2).

These results from the GCB indicate a progression of biomineralizing phytoplankton southwards during spring as irradiance conditions become optimal and macronutrients are depleted. Low silicic acid is often associated with a

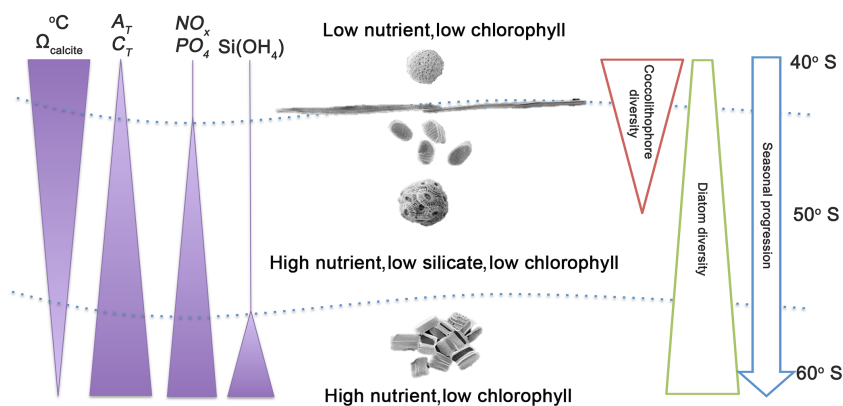


Figure 6. Schematic of the potential seasonal progression occurring in the Great Calcite Belt, allowing coccolithophores to develop after the main diatom bloom. Note that phytoplankton example images are not to scale.

high residual nitrate concentration (defined as $[\text{NO}_3^-] - [\text{Si}(\text{OH})_4]$), as has been observed on the Patagonian Shelf (Balch et al., 2014). The highest coccolithophore abundances in this study (excluding the Patagonian Shelf) were observed in regions with “residual nitrate” concentrations greater than $10 \mu\text{M}$ (Balch et al., 2016). As silicic acid becomes depleted in the more northerly surface waters in spring, diatoms progressively become more successful further south as irradiance conditions allow, thereby producing a large HNLSiLC area between the Subantarctic Front and the Polar Front; an ideal environment for late-summer *E. huxleyi* communities to develop (Fig. 6).

Dissolved iron (dFe) acts as a strong control on phytoplankton growth, community composition, and species biogeography (e.g., Boyd, 2002; Boyd et al., 2015). In this study, dFe measurements were only made at a small number of sampling stations ($n = 6$; Twining, unpublished data; Balch et al., 2016), limiting their use in the multivariate statistical analysis of community composition. For these stations, dFe showed a statistically significant negative correlation (Pearson’s product moment = -0.957 , $p < 0.01$) with PC2 from the environmental analysis (Fig. S2). PC2 described the environmental variables least related to latitude (pH, $p\text{CO}_2$ and \bar{E}_{MLD}), indicating that dFe was also decoupled from the strong latitudinal gradient in environmental parameters (i.e., SST, Ω_{calcite} , macronutrients) in austral spring–summer. Interestingly, dFe concentrations positively correlated with coccolithophore abundance (Pearson’s product moment correlation = 0.858 , $p < 0.05$) rather than diatom abundance ($p = 0.132$, ns) (Fig. S2). Overall, these data support the hypothesis that coccolithophores occupy a niche unoccupied by large diatoms when dFe is replete and silicic acid is depleted (Balch et al., 2014; Hopkins et al., 2015). The numerical dominance of small diatoms less than $20 \mu\text{m}$ in the GCB during austral spring and summer, alongside the coccolithophore *E. huxleyi*, is thus potentially due to the reduced impact of nutrient limitation (dFe, silicic acid) on small cells with high

ratios of surface area to volume (e.g., Hinz et al., 2012; Balch et al., 2014).

4.4 Relating the Great Calcite Belt to carbonate chemistry

Relating carbonate chemistry to phytoplankton distribution, growth, and physiology is an important step when considering the potential effects of climate change and ocean acidification on marine biogeochemistry. In this study, no significant correlation (Spearman’s $r = 0.259$, $p = 0.164$, $n = 27$) occurred between pH and Chl *a*. The inclusion of $p\text{CO}_2$ and Ω_{calcite} as influential factors in the statistical results describing GCB species biogeography highlights the importance of understanding phytoplankton responses to carbonate chemistry as a whole rather than as individual carbonate chemistry parameters (Bach et al., 2015). Of the four major species driving the differences in biomineralizing plankton community composition and biogeography across the GCB, only *F. pseudonana* abundance was positively correlated with $p\text{CO}_2$ (Pearson’s product moment coefficient = 0.577 , $p < 0.05$, $n = 16$).

The response of diatoms to increasing $p\text{CO}_2$ is not straightforward (e.g., Boyd et al., 2015), with some studies implying that large diatoms may be more successful in future climate scenarios (e.g., Tortell et al., 2008; Flynn et al., 2012), although changes in nutrient and light availability (via stronger stratification) may prevent a permanent switch in phytoplankton community structure (Bopp et al., 2005). The carbonate chemistry system is complex, as biological activity also impacts the concentration of each of the components. Organic matter production reduces total dissolved inorganic carbon (C_T), and hence $p\text{CO}_2$ via photosynthesis, and increases alkalinity (A_T) through nutrient uptake, while subsequent respiration and remineralization of organic matter has the opposite impact. The simultaneous actions of biological and physical processes result in seasonal and localized

changes in the carbonate system, which are often difficult to decouple.

In our study, there was no significant correlation between *E. huxleyi* and Ω_{calcite} (Pearson's product moment = 0.093). However, the waters of the GCB remained oversaturated ($\Omega_{\text{calcite}} > 2$) throughout, and the relationship between coccolithophores, calcification, and carbonate chemistry is now recognized as being complex and nonlinear (e.g., Beaufort et al., 2011; Smith et al., 2012; Poulton et al., 2014; Rivero-Calle et al., 2015; Bach et al., 2015; Charalampopoulou et al., 2016; Marañón et al., 2016). Hence, significant gaps remain in our understanding of the in situ coccolithophore response to increasing $p\text{CO}_2$, reduced pH, or decreasing Ω_{calcite} . Notably, a significant positive correlation between *Pseudo-nitzschia* spp. and Ω_{calcite} also existed (Pearson's product moment correlation = 0.5924, $p < 0.01$, $n = 19$) across the GCB despite there being no presently known detrimental effect on diatoms with low saturation states. However, due to the tight coupling of temperature and Ω_{calcite} (and *Pseudo-nitzschia* spp. and temperature), the correlation is more likely to be temperature driven.

5 Summary

This study of the GCB further highlights the importance of understanding the environmental controls on the distribution of biomineralizing nanoplankton in the Southern Ocean. The results of this study suggest that three nanophytoplankton ($< 20 \mu\text{m}$) and one microphytoplankton ($> 20 \mu\text{m}$) species (three diatoms and one coccolithophore; *F. pseudonana*, *F. nana*, *Pseudo-nitzschia* spp., and *Emiliania huxleyi*) numerically dominated the compositional variation in biomineralizing phytoplankton biogeography across the GCB. The contribution of *E. huxleyi* to phytoplankton biomass (as estimated from cell counts and Chl *a*) was generally less than 5%, although it increased to 20% in association with high-reflectance PIC features found on the Patagonian Shelf, north of South Georgia in the South Atlantic Ocean, and north of the Crozet Islands in the southern Indian Ocean. This indicates that in the post-spring bloom conditions of the GCB, *E. huxleyi* is an important contributor to phytoplankton biomass and primary production at localized spatial scales.

Out of a wide suite of environmental variables, latitudinal gradients in temperature, macronutrients, $p\text{CO}_2$, and Ω_{calcite} “best” statistically described the variation in the phytoplankton community composition in this study, whereas \bar{E}_{MLD} and pH did not rank as significant factors influencing species composition. However, not all species were directly sensitive to the same environmental gradients determined to be influencing the overall biogeography. The negative correlation between *E. huxleyi* and silicic acid highlights the potential for a seasonal southward movement of *E. huxleyi* once diatom blooms have depleted silicic acid.

These results highlight the fact that the Southern Ocean is a highly dynamic system and further studies examining environmental controls on community distribution earlier in the productive season would greatly enhance the overall understanding of the progression of phytoplankton community biogeography. The phytoplankton dynamics of the GCB are also more complex than first considered, with nanophytoplankton (e.g., *F. pseudonana*) numerically dominant in non-bloom conditions (as opposed to microphytoplankton), which has further implications for modeling carbon export and projecting phytoplankton changes in future oceanic scenarios.

Data availability. The coccolithophore and diatom abundance data can be accessed via the PANGAEA database: <https://doi.org/10.1594/PANGAEA.879790> (Smith et al., 2017).

The Supplement related to this article is available online at <https://doi.org/10.5194/bg-14-4905-2017-supplement>.

Competing interests. The authors declare that they have no conflict of interest.

Acknowledgements. We would like to thank all the scientists, officers, and crew onboard the R/V *Melville* and R/V *Revelle*, and Matt Durham (Scripps Institution of Oceanography) in particular. Nutrient and salinity data are presented courtesy of the Oceanographic Data Facility, Scripps Institute of Oceanography (ODF/SIO) with thanks to shipboard technicians Melissa Miller and John Calderwood. The GCB cruises were supported by the National Science Foundation (OCE-0961660 to William M. Balch and Ben S. Twining, OCE-0728582 to William M. Balch, OCE-0961414 to Nicholas R. Bates) and National Aeronautics and Space Administration (NNX11AO72G, NNX11AL93G, NNX14AQ41G, NNX14AQ43A, NNX14AL92G, and NNX14AM77G to William M. Balch). Helen E. K. Smith and Alex J. Poulton were supported by the Natural Environmental Research Council (NERC), including a NERC Fellowship to Alex J. Poulton (NE/F015054/1) and the UK Ocean Acidification Research Programme (NE/H017097/1) with a tied studentship to Helen E. K. Smith and an added value award to Alex J. Poulton.

Edited by: Koji Suzuki

Reviewed by: three anonymous referees

References

- Armand, L. K., Cornet-Barthaux, V., Mosseri, J., and Quéguiner, B.: Late summer diatom biomass and community structure on and around the naturally iron-fertilised Kerguelen Plateau in the Southern Ocean, *Deep Sea-Res. Pt. II*, 55, 653–676, <https://doi.org/10.1016/j.dsr2.2007.12.031>, 2008.
- Arrigo, K. R., Worthen, D., Schnell, A., and Lizotte, M. P.: Primary production in Southern Ocean waters, *J. Geophys. Res.*, 103, 151587–15600, 1998.
- Assmy, P., Smetacek, V., Montresor, M., Klaas, C., Henjes, J., Strass, V. H., Arrieta, J. M., Bathmann, U., Berg, G. M., Breibarth, E., Cisewski, B., Friedrichs, L., Fuchs, N., Herndl, G. J., Jansen, S., Krägersky, S., Latasa, M., Peeken, I., Röttgers, R., Scharek, R., Schüller, S. E., Steigenberger, S., Webb, A., and Wolf-Gladrow, D.: Thick-shelled, grazer-protected diatoms decouple ocean carbon and silicon cycles in the iron-limited Antarctic Circumpolar Current, *P. Natl. Acad. Sci. USA.*, 110, 20633–20638, <https://doi.org/10.1073/pnas.1309345110>, 2013.
- Bach, L. T., Riebesell, U., Gutowska, M. A., Federwisch, L., and Schulz, K. G.: A unifying concept of coccolithophore sensitivity to changing carbonate chemistry embedded in an ecological framework, *Prog. Oceanogr.*, 135, 125–138, 2015.
- Baines, S. B., Twining, B. S., Brzezinski, M. A., Nelson, D. M., and Fisher, N. S.: Causes and biogeochemical implications of regional differences in silicification of marine diatoms, *Global Biogeochem. Cy.*, 24, 1–15, <https://doi.org/10.1029/2010GB003856>, 2010.
- Balch, W. M., Gordon, H. R., Bowler, B. C., Drapeau, D. T., and Booth, E. S.: Calcium carbonate measurements in the surface global ocean based on Moderate-Resolution Imaging Spectroradiometer data, *J. Geophys. Res.-Oceans*, 110, C07001, <https://doi.org/10.1029/2004JC002560>, 2005.
- Balch, W. M., Bowler, B. C., Drapeau, D. T., Poulton, A. J., and Holligan, P. M.: Biominerals and the vertical flux of particulate organic carbon from the surface ocean, *Geophys. Res. Lett.*, 37, 1–6, <https://doi.org/10.1029/2010GL044640>, 2010.
- Balch, W. M., Drapeau, D. T., Bowler, B. C., Lyczskowski, E., Booth, E. S., and Alley, D.: The contribution of coccolithophores to the optical and inorganic carbon budgets during the Southern Ocean Gas Exchange Experiment: New evidence in support of the “Great Calcite Belt”; hypothesis, *J. Geophys. Res.*, 116, C00F06, <https://doi.org/10.1029/2011JC006941>, 2011.
- Balch, W. M., Drapeau, D. T., Bowler, B. C., Lyczskowski, E. R., Lubelczyk, L. C., Painter, S. C., and Poulton, A. J.: Surface biological, chemical, and optical properties of the Patagonian Shelf coccolithophore bloom, the brightest waters of the Great Calcite Belt, *Limnol. Oceanogr.*, 59, 1715–1732, <https://doi.org/10.4319/lo.2014.59.5.1715>, 2014.
- Balch, W. M., Bates, N. R., Lam, P. J., Twining, B. S., Rosengard, S. Z., Bowler, B. C., Drapeau, D. T., Garley, R., Lubelczyk, L. C., Mitchell, C., and Rauschenberg, S.: Factors regulating the Great Calcite Belt in the Southern Ocean and its biogeochemical significance, *Global Biogeochem. Cy.*, 30, 1124–1144, <https://doi.org/10.1002/2016GB005414>, 2016.
- Barber, R. T. and Hiscock, M. R.: A rising tide lifts all phytoplankton: Growth response of other phytoplankton taxa in diatom-dominated blooms, *Global Biogeochem. Cy.*, 20, GB4S03, <https://doi.org/10.1029/2006GB002726>, 2006.
- Bates, N. R., Michaels, A. F., and Knap, A. H.: Seasonal and interannual variability of oceanic carbon dioxide species at US JGOFS Bermuda Atlantic Time-series Study (BATS) site, *Deep-Sea Res. Pt. II*, 43, 347–383, 1996.
- Bates, N. R., Best, M. H. P., Neely, K., Garley, R., Dickson, A. G., and Johnson, R. J.: Detecting anthropogenic carbon dioxide uptake and ocean acidification in the North Atlantic Ocean, *Biogeosciences*, 9, 2509–2522, <https://doi.org/10.5194/bg-9-2509-2012>, 2012.
- Bathmann, U., Scharek, R., Klaas, C., Dubischar, C., and Smetacek, V.: Spring development of phytoplankton biomass and composition in major water masses of the Atlantic sector of the Southern Ocean, *Deep-Sea Res. Pt. II*, 44, 51–67, 1997.
- Beaufort, L., Probert, I., de Garidel-Thoron, T., Bendif, E. M., Ruiz-Pino, D., Metzl, N., Goyet, C., Buchet, N., Coupel, P., Grelaud, M., Rost, B., Rickaby, R. E. M., and de Vargas, C.: Sensitivity of coccolithophores to carbonate chemistry and ocean acidification, *Nature*, 476, 80–88, <https://doi.org/10.1038/nature10295>, 2011.
- Belkin, I. M. and Gordon, A. L.: Southern Ocean fronts from the Greenwich meridian to Tasmania, *J. Geophys. Res.*, 101, 3675–3696, <https://doi.org/10.1029/95JC02750>, 1996.
- Bopp, L., Monfray, P., Aumont, O., Dufresne, J.-L., Le Treut, H., Madec, G., Terray, L., and Orr, J. C.: Potential impact of climate change on marine export production, *Global Biogeochem. Cy.*, 15, 81–99, <https://doi.org/10.1029/1999GB001256>, 2001.
- Bopp, L., Aumont, O., Cadule, P., Alvain, S., and Gehlen, M.: Response of diatoms distribution to global warming and potential implications: A global model study, *Geophys. Res. Lett.*, 32, L19606, <https://doi.org/10.1029/2005GL023653>, 2005.
- Boyd, P. W.: Environmental factors controlling phytoplankton processes in the Southern Ocean, *J. Phycol.*, 38, 844–861, 2002.
- Boyd, P. W. and Newton, P. P.: Does planktonic community structure determine downward particulate organic carbon flux in different oceanic provinces?, *Deep-Sea Res. Pt. I*, 46, 63–91, [https://doi.org/10.1016/S0967-0637\(98\)00066-1](https://doi.org/10.1016/S0967-0637(98)00066-1), 1999.
- Boyd, P. W., Strzepek, R., Fu, F., and Hutchins, D. A.: Environmental control of open-ocean phytoplankton groups: Now and in the future, *Limnol. Oceanogr.*, 55, 1353–1376, <https://doi.org/10.4319/lo.2010.55.3.1353>, 2010.
- Boyd, P. W., Arrigo, K. R., Strzepek, R., and van Dijken, G. L.: Mapping phytoplankton iron utilization: Insights into Southern Ocean supply mechanisms, *J. Geophys. Res.-Oceans*, 117, C06009, <https://doi.org/10.1029/2011JC007726>, 2012.
- Boyd, P. W., Lennartz, S. T., Glover, D. M., and Doney, S. C.: Biological ramifications of climate-change-mediated oceanic multi-stressors, *Nat. Clim. Change*, 5, 71–79, <https://doi.org/10.1038/NCLIMATE2441>, 2015.
- Caldeira, K. and Wickett, M.: Anthropogenic carbon and ocean pH, *Nature*, 425, 365, <https://doi.org/10.1038/425365a>, 2003.
- Charalampopoulou, A., Poulton, A. J., Tyrrell, T., and Lucas, M. I.: Irradiance and pH affect coccolithophore community composition on a transect between the North Sea and the Arctic Ocean, *Mar. Ecol.-Prog. Ser.*, 431, 25–43, <https://doi.org/10.3354/meps09140>, 2011.
- Charalampopoulou, A., Poulton, A. J., Bakker, D. C. E., Lucas, M. I., Stinchcombe, M. C., and Tyrrell, T.: Environmental drivers of coccolithophore abundance and calcification across Drake Passage (Southern Ocean), *Biogeosciences*, 13, 5917–5935, <https://doi.org/10.5194/bg-13-5917-2016>, 2016.

- Clarke, K. R.: Non-parametric multivariate analyses of changes in community structure, *Aust. J. Ecol.*, 18, 117–143, 1993.
- Clarke, K. R. and Gorley, R. N.: PRIMER v6: user manual/tutorial, PRIMER v6., PRIMER-E, Plymouth, 2006.
- Clarke, K. R. and Warwick, R. M.: Change in Marine Communities: An Approach to Statistical Analysis and Interpretation, 2nd Edn., PRIMER-E, Plymouth, 2001.
- Clarke, K. R., Somerfield, P. J., and Gorley, R. N.: Testing of null hypotheses in exploratory community analyses: similarity profiles and biota-environment linkage, *J. Exp. Mar. Biol. Ecol.*, 366, 56–69, 2008.
- Cook, S. S., Whittock, L., Wright, S. W., and Hallegraeff, G. M.: Photosynthetic pigment and genetic differences between two Southern Ocean morphotypes of *Emiliana huxleyi* (Haptophyta)1, *J. Phycol.*, 47, 615–626, <https://doi.org/10.1111/j.1529-8817.2011.00992.x>, 2011.
- Cook, S. S., Jones, R. C., Vaillancourt, R. E., and Hallegraeff, G. M.: Genetic differentiation among Australian and Southern Ocean populations of the ubiquitous coccolithophore *Emiliana huxleyi* (Haptophyta), *Phycologia*, 52, 368–374, <https://doi.org/10.2216/12-111.1>, 2013.
- Cubillos, J., Wright, S., Nash, G., de Salas, M., Griffiths, B., Tilbrook, B., Poisson, A., and Hallegraeff, G.: Calcification morphotypes of the coccolithophorid *Emiliana huxleyi* in the Southern Ocean: changes in 2001 to 2006 compared to historical data, *Mar. Ecol.-Prog. Ser.*, 348, 47–54, <https://doi.org/10.3354/meps07058>, 2007.
- Daniels, C. J., Sheward, R. M., and Poulton, A. J.: Biogeochemical implications of comparative growth rates of *Emiliana huxleyi* and *Coccolithus species*, *Biogeosciences*, 11, 6915–6925, <https://doi.org/10.5194/bg-11-6915-2014>, 2014.
- de Baar, H. J. W., Boyd, P. W., Coale, K. H., Landry, M. R., Tsuda, A., Assmy, P., Bakker, D. C. E., Bozec, Y., Barber, R. T., Brzezinski, M. A., Buesseler, K. O., Boye, M., Croot, P., Gervais, F., Gorbunov, M., Harrison, P. J., Hiscock, W. T., Laan, P., Lancelot, C., Law, C. S., Levasseur, M., Marchetti, A., Millero, F. J., Nishioka, J., Nojirim, Y., van Oijen, T., Riebesell, U., Rijkenberg, M. J. A., Saito, H., Takeda, S., Timmermans, K. R., Veldhuis, M. J. W., Waite, A. M., and Wong, C. S.: Synthesis of iron fertilization experiments: From the Iron Age in the Age of Enlightenment, *J. Geophys. Res.*, 110, C09S16, <https://doi.org/10.1029/2004JC002601>, 2005.
- Deppeler, S. L. and Davidson, A. T.: Southern Ocean phytoplankton in a changing climate, *Front. Mar. Sci.*, 4, 40, <https://doi.org/10.3389/fmars.2017.00040>, 2017.
- Dickson, A. G. and Millero, F. J.: A comparison of the equilibrium constants for the dissociation of carbonic acid in seawater media, *Deep-Sea Res.*, 36, 1733–1743, 1987.
- Doney, S. C., Fabry, V. J., Feely, R. A., and Kleympas, J. A.: Ocean acidification: the other CO₂ problem, *Annu. Rev. Mar. Sci.*, 1, 169–192, <https://doi.org/10.1146/annurev.marine.010908.163834>, 2009.
- Dugdale, R. C., Wilkerson, F. P., and Minas, H. J.: The role of a silicate pump in driving new production, *Deep-Sea Res. Pt. I*, 42, 697–719, 1995.
- Durak, G. M., Taylor, A. R., Probert, I., de Vargas, C., Audic, S., Schroeder, D. C., Brownlee, C., and Wheeler, G. L.: A role for diatom-like silicon transporters in calcifying coccolithophores, *Nat. Commun.*, 7, 10543, <https://doi.org/10.1038/ncomms10543>, 2016.
- Edge, J. K. and Asknes, D. L.: Silicate as a regulating nutrient in phytoplankton competition, *Mar. Ecol.-Prog. Ser.*, 83, 281–289, 1992.
- Eynaud, F., Giraudeau, J., Pichon, J.-J., and Pudsey, C. J.: Sea-surface distribution of coccolithophores, diatoms, silicoflagellates and dinoflagellates in the South Atlantic Ocean during the late austral summer 1995, *Deep-Sea Res. Pt. I*, 46, 451–482, [https://doi.org/10.1016/S0967-0637\(98\)00079-X](https://doi.org/10.1016/S0967-0637(98)00079-X), 1999.
- Flynn, K. J. K., Blackford, J. J. C., Baird, M. E. M., Raven, J. A., Clark, D. R., Beardall, J., Brownlee, C., Fabian, H., and Wheeler, G. L.: Changes in pH at the exterior surface of plankton with ocean acidification, *Nat. Clim. Change*, 2, 510–513, <https://doi.org/10.1038/nclimate1489>, 2012.
- Froneman, P. W., McQuaid, C. D., and Perissinotto, R.: Biogeographic structure of the microphytoplankton assemblages of the South Atlantic and Southern Ocean during austral summer, *J. Plankton Res.*, 17, 1791–1802, <https://doi.org/10.1093/plankt/17.9.1791>, 1995.
- Froneman, P. W., Pakhomov, E. A., and Balarin, M. G.: Size-fractionated phytoplankton biomass, production and biogenic carbon flux in the eastern Atlantic sector of the Southern Ocean in late austral summer 1997–1998, *Deep-Sea Res. Pt. II*, 51, 2715–2729, 2004.
- Gall, M. P., Boyd, P. W., Hall, J., Safi, K. A., and Chang, H.: Phytoplankton processes. Part 1: Community structure during the Southern Ocean Iron RElease Experiment (SOIREE), *Deep-Sea Res. Pt. II*, 48, 2551–2570, 2001.
- Garcia, C. A. E., Garcia, V. M. T., Dogliotti, A. I., Ferreira, A., Romero, S. I., Mannino, A., Souza, M. S., and Mata, M. M.: Environmental conditions and bio-optical signature of a coccolithophorid bloom in the Patagonian shelf, *J. Geophys. Res.-Oceans*, 116, 1–17, <https://doi.org/10.1029/2010JC006595>, 2011.
- Grigorov, I. and Rigual-Hernandez, A.: Settling fluxes of diatoms to the interior of the Antarctic circumpolar current along 170°W, *Deep-Sea Res. Pt. I*, 93, 1–13, <https://doi.org/10.1016/j.dsr.2014.07.008>, 2014.
- Hasle, G. R. and Syvertsen, E. E.: Chapter 2 – Marine Diatoms, in: *Marine Phytoplankton*, edited by: Tomas, C. R., 5–385, Academic Press, San Diego, 1997.
- Haxo, F. T.: Photosynthetic action spectrum of the coccolithophorid, *Emiliana huxleyi* (Haptophyceae): 19' hexanoyloxyfucoxanthin as antenna pigment, *J. Phycol.*, 21, 282–287, 1985.
- Hinz, D. J., Poulton, A. J., Nielsdóttir, M. C., Steigenberger, S., Korb, R. E., Achterberg, E. P., and Bibby, T. S.: Comparative seasonal biogeography of mineralising nanoplankton in the Scotia Sea: *Emiliana huxleyi*, *Fragilariopsis* spp. and *Tetraparma pelagica*, *Deep-Sea Res. Pt. II*, 59–60, 57–66, <https://doi.org/10.1016/j.dsr.2011.09.002>, 2012.
- Ho, T., Quigg, A., Finkel, Z. V., Milligan, A. J., Wyman, K., Falkowski, P. G., and Morel, M. M.: The elemental composition of some marine phytoplankton, *J. Phycol.*, 1159, 1145–1159, 2003.
- Holligan, P. M., Charalampopoulou, A., and Hutson, R.: Seasonal distributions of the coccolithophore, *Emiliana huxleyi*, and of particulate inorganic carbon in surface waters of the Scotia Sea, *J. Marine Syst.*, 82, 195–205, 2010.

- Honjo, S., Francois, R., Manganini, S., and Dymond, J.: Particle fluxes to the interior of the Southern Ocean in the Western Pacific sector along 170° W, *Deep-Sea Res.*, 47, 3521–3548, [https://doi.org/10.1016/S0967-0645\(00\)00077-1](https://doi.org/10.1016/S0967-0645(00)00077-1), 2000.
- Hopkins, J., Henson, S. A., Painter, S. C., Tyrrell, T., and Poulton, A. J.: Phenological characteristics of coccolithophore blooms, *Global Biogeochem. Cy.*, 29, 239–253, <https://doi.org/10.1002/2014GB004919>, 2015.
- Knap, A. H., Michaels, A., Close, A. R., Ducklow, H., and Dickson, A. G.: Protocols for the joint global ocean flux study (JGOFS) core measurements, JGOFS Repr IOC Man Guid No 29 UNESCO 1994, 1996.
- Kopczynska, E. E., Weber, L. H., and El-Sayed, S. Z.: Phytoplankton species composition and abundance in the Indian Sector of the Antarctic Ocean, *Polar Biol.*, 6, 161–169, 1986.
- Kopczynska, E. E., Fiala, M., and Jeandel, C.: Annual and inter-annual variability in phytoplankton at a permanent station off Kerguelen Islands, Southern Ocean, *Polar Biol.*, 20, 342–351, <https://doi.org/10.1007/s003000050312>, 1998.
- Korb, R. E., Whitehouse, M. J., Atkinson, A., and Thorpe, S. E.: Magnitude and maintenance of the phytoplankton bloom at South Georgia: a naturally iron-replete environment, *Mar. Ecol.-Prog. Ser.*, 368, 75–91, <https://doi.org/10.3354/meps07525>, 2008.
- Korb, R. E., Whitehouse, M. J., Gordon, M., Ward, P., and Poulton, A. J.: Summer microplankton community structure across the Scotia Sea: implications for biological carbon export, *Biogeosciences*, 7, 343–356, <https://doi.org/10.5194/bg-7-343-2010>, 2010.
- Korb, R. E., Whitehouse, M. J., Ward, P., Gordon, M., Venables, H. J., and Poulton, A. J.: Regional and seasonal differences in microplankton biomass, productivity, and structure across the Scotia Sea: Implications for the export of biogenic carbon, *Deep-Sea Res. Pt. II*, 59–60, 67–77, <https://doi.org/10.1016/j.dsr2.2011.06.006>, 2012.
- Langer, G., Geisen, M., Baumann, K.-H., Kläs, J., Riebesell, U., Thoms, S., and Young, J. R.: Species-specific responses of calcifying algae to changing seawater carbonate chemistry, *Geochem. Geophys. Geosys.*, 7, Q09006, <https://doi.org/10.1029/2005GC001227>, 2006.
- Langer, G., Probert, I., Nehrke, G., and Ziveri, P.: The morphological response of *Emiliania huxleyi* to seawater carbonate chemistry changes: an inter-strain comparison, *J. Nannoplankton Res.*, 32, 29–34, 2011.
- Leblanc, K., Hare, C. E., Boyd, P. W., Bruland, K. W., Sohst, B., Pickmere, S., Lohan, M. C., Buck, K., Ellwood, M., and Hutchins, D. A.: Fe and Zn effects on the Si cycle and diatom community structure in two contrasting high and low-silicate HNLC areas, *Deep-Sea Res. Pt. I*, 52, 1842–1864, <https://doi.org/10.1016/j.dsr.2005.06.005>, 2005.
- Leblanc, K., Hare, C. E., Feng, Y., Berg, G. M., DiTullio, G. R., Neeley, A., Benner, I., Sprengel, C., Beck, A., Sanudo-Wilhelmy, S. A., Passow, U., Klinck, K., Rowe, J. M., Wilhelm, S. W., Brown, C. W., and Hutchins, D. A.: Distribution of calcifying and silicifying phytoplankton in relation to environmental and biogeochemical parameters during the late stages of the 2005 North East Atlantic Spring Bloom, *Biogeosciences*, 6, 2155–2179, <https://doi.org/10.5194/bg-6-2155-2009>, 2009.
- Leblanc, K., Arístegui, J., Armand, L., Assmy, P., Beker, B., Bode, A., Breton, E., Cornet, V., Gibson, J., Gosselin, M.-P., Kopczynska, E., Marshall, H., Peloquin, J., Piontkovski, S., Poulton, A. J., Quéguiner, B., Schiebel, R., Shipe, R., Stefels, J., van Leeuwe, M. A., Varela, M., Widdicombe, C., and Yallop, M.: A global diatom database – abundance, biovolume and biomass in the world ocean, *Earth Syst. Sci. Data*, 4, 149–165, <https://doi.org/10.5194/essd-4-149-2012>, 2012.
- Le Moigne, F. A. C., Sanders, R. J., Villa-Alfageme, M., Martin, A. P., Pabortsava, K., Planquette, H., Morris, P. J., and Thomalla, S. J.: On the proportion of ballast versus non-ballast associated carbon export in the surface ocean, *Geophys. Res. Lett.*, 39, L15610, <https://doi.org/10.1029/2012GL052980>, 2012.
- Le Moigne, F. A. C., Boye, M., Masson, A., Corvaisier, R., Grossteffan, E., Guéneugues, A., and Pondaven, P.: Description of the biogeochemical features of the subtropical southeastern Atlantic and the Southern Ocean south of South Africa during the austral summer of the International Polar Year, *Biogeosciences*, 10, 281–295, <https://doi.org/10.5194/bg-10-281-2013>, 2013.
- Lewis, E. and Wallace, D. W. R.: Program Developed for CO₂ System Calculations Rep. ORNL/CDIAC-105, Carbon Dioxide Information Analysis Center, Oak Ridge National Laboratory, U.S. Department of Energy, Oak Ridge, Tennessee, 1998.
- Marañón, E., Balch, W. M., Cermeño, P., González, N., Sobrino, C., Fernández, A., Huete-Ortega, M., López-Sandoval, D. C., Delgado, M., Estrada, M., Álvarez, M., Fernández-Guallart, E., and Pelejero, C.: Coccolithophore calcification is independent of carbonate chemistry in the tropical ocean, *Limnol. Oceanogr.*, 61, 1345–1357, <https://doi.org/10.1002/lno.10295>, 2016.
- Martin, J. H., Fitzwater, S. E., and Gordon, R. M.: Iron deficiency limits phytoplankton growth in Antarctic waters, *Global Biogeochem. Cy.*, 4, 5–12, <https://doi.org/10.1029/GB0041001p00005>, 1990.
- Mehrbach, C., Culbertson, C. H., Hawley, J. E., and Pytkowicz, R. M.: Measurement of the apparent dissociation constants of carbonic acid in seawater at atmospheric pressure, *Limnol. Oceanogr.*, 18, 897–907, 1973.
- Mohan, R., Mergulhao, L. P., Guptha, M. V. S., Rajakumar, A., Thamban, M., AnilKumar, N., Sudhakar, M., and Ravindra, R.: Ecology of coccolithophores in the Indian sector of the Southern Ocean, *Mar. Micropaleontol.*, 67, 30–45, <https://doi.org/10.1016/j.marmicro.2007.08.005>, 2008.
- Moore, C. M., Hickman, A. E., Poulton, A. J., Seeyave, S., and Lucas, M. I.: Iron–light interactions during the CROZet natural iron bloom and EXport experiment (CROZEX): II – Taxonomic responses and elemental stoichiometry, *Deep-Sea Res. Pt. II*, 54, 2066–2084, <https://doi.org/10.1016/j.dsr2.2007.06.015>, 2007.
- Nelson, D. and Tréguer, P.: Role of silicon as a limiting nutrient to Antarctic diatoms: Evidence from kinetic studies in the Ross Sea ice-edge zone, *Mar. Ecol.-Prog. Ser.*, 80, 255–264, 1992.
- Orsi, A. H., Whitworth, T., and Nowlin Jr., W. D.: On the meridional extent and fronts of the Antarctic Circumpolar Current, *Deep-Sea Res. Pt. I*, 42, 641–673, 1995.
- Paasche, E.: Silicon and the ecology of marine planktonic diatoms. 1. *Thalassiosira pseudonana* (*Cyclotella nana*) grown in chemostats with silicate as the limiting nutrient, *Mar. Biol.*, 19, 117–126, 1973a.

- Paasche, E.: Silicon and the ecology of marine plankton diatoms. II. Silicate-uptake kinetics in five diatom species, *Mar. Biol.*, 19, 262–269, 1973b.
- Paasche, E.: A review of the coccolithophorid *Emiliania huxleyi* (Prymnesiophyceae), with particular reference to growth, coccolith formation, and calcification-photosynthesis interactions, *Phycologia*, 40, 503–529, 2001.
- Painter, S. C., Poulton, A. J., Allen, J. T., Pidcock, R., and Balch, W. M.: The COPAS08 expedition to the Patagonian Shelf: Physical and environmental conditions during the 2008 coccolithophore bloom, *Cont. Shelf Res.*, 30, 1907–1923, <https://doi.org/10.1016/j.csr.2010.08.013>, 2010.
- Petrou, K., Kranz, S. A., Trimborn, S., Hassler, C. S., Blanco, S., Sackett, O., Ralph, P. J., and Davidson, A. T.: Southern Ocean phytoplankton physiology in a changing climate, *J. Plant Physiol.*, 203, 135–150, <https://doi.org/10.1016/j.jplph.2016.05.004>, 2016.
- Pondaven, P., Ragueneau, O., Tréguer, P., Hauvespre, A., Dezileau, L., and Reyss, J.: Resolving the “opal paradox” in the Southern Ocean, *Nature*, 405, 168–72, <https://doi.org/10.1038/35012046>, 2000.
- Poulton, A. J., Mark Moore, C., Seeyave, S., Lucas, M. I., Fielding, S., and Ward, P.: Phytoplankton community composition around the Crozet Plateau, with emphasis on diatoms and *Phaeocystis*, *Deep-Sea Res. Pt. II*, 54, 2085–2105, <https://doi.org/10.1016/j.dsr2.2007.06.005>, 2007.
- Poulton, A. J., Charalampopoulou, A., Young, J. R., Tarran, G. A., Lucas, M. I., and Quartly, G. D.: Coccolithophore dynamics in non-bloom conditions during late summer in the central Iceland Basin (July–August 2007), *Limnol. Oceanogr.*, 55, 1601–1613, 2010.
- Poulton, A. J., Young, J. R., Bates, N. R., and Balch, W. M.: Biometry of detached *Emiliania huxleyi* coccoliths along the Patagonian Shelf, *Mar. Ecol.-Prog. Ser.*, 443, 1–17, <https://doi.org/10.3354/meps09445>, 2011.
- Poulton, A. J., Painter, S. C., Young, J. R., Bates, N. R., Bowler, B., Drapeau, D., Lyczszkowski, E., and Balch, W. M.: The 2008 *Emiliania huxleyi* bloom along the Patagonian Shelf: Ecology, biogeochemistry, and cellular calcification, *Global Biogeochem. Cy.*, 27, 1023–1033, <https://doi.org/10.1002/2013GB004641>, 2013.
- Poulton, A. J., Stinchcombe, M. C., Achterberg, E. P., Bakker, D. C. E., Dumousseaud, C., Lawson, H. E., Lee, G. A., Richier, S., Suggett, D. J., and Young, J. R.: Coccolithophores on the north-west European shelf: calcification rates and environmental controls, *Biogeosciences*, 11, 3919–3940, <https://doi.org/10.5194/bg-11-3919-2014>, 2014.
- Poulton, A. J., Holligan, P. M., Charalampopoulou, A., and Adey, T.R.: Coccolithophore ecology in the tropical and subtropical Atlantic Ocean: New perspectives from the Atlantic meridional transect (AMT) programme, *Prog. Oceanogr.*, <https://doi.org/10.1016/j.pocan.2017.01.003>, 2017.
- Raven, J. A. and Geider, R. J.: Temperature and algal growth, *New Phytol.*, 110, 441–461, 1988.
- Read, J. F., Pollard, R. T., and Allen, J. T.: Sub-mesoscale structure and the development of an eddy in the Subantarctic Front north of the Crozet Islands, *Deep-Sea Res. Pt. II*, 54, 1930–1948, <https://doi.org/10.1016/j.dsr2.2007.06.013>, 2007.
- Rivero-Calle, S., Gnanadesikan, A., Del Castillo, C. E., Balch, W. M., and Guikema, S. D.: Multidecadal increase in North Atlantic coccolithophores and the potential role of rising CO₂, *Science*, 350, 1533–1537, 2015.
- Robbins, L. L., Hansen, M. E., Kleypas, J. A., and Meylan, S. C.: CO₂calc: A user-friendly seawater carbon calculator for Windows, Mac OS X, and iOS (iPhone)Rep., 17 pp., US Geological Survey, Reston, VA, USA, 2010.
- Sabine, C. L., Feely, R. A., Gruber, N., Key, R. M., Lee, K., Bullister, J. L., Wanninkhof, R., Wong, C. S., Wallace, D. W. R., Tilbrook, B., Millero, F. J., Peng, T.-H., Kozyr, A., Ono, T., and Rios, A. F.: The Oceanic Sink for Anthropogenic CO₂, *Science*, 305, 367–371, <https://doi.org/10.1126/science.1097403>, 2004.
- Salter, I., Lampitt, R. S., Sanders, R., Poulton, A., Kemp, A. E. S., Boorman, B., Saw, K., and Pearce, R.: Estimating carbon, silica and diatom export from a naturally fertilised phytoplankton bloom in the Southern Ocean using PELAGRA: A novel drifting sediment trap, *Deep-Sea Res. Pt. II*, 54, 2233–2259, 2007.
- Sarmiento, J. L., Hughes, T. M. C., Stouffer, R. J., and Manabe, S.: Simulated response of the ocean carbon cycle to anthropogenic climate warming, *Nature*, 393, 245–249, 1998.
- Sarmiento, J. L., Slater, R., Barber, R., Bopp, L., Doney, S. C., Hirst, A. C., Kleypas, J., Matear, R., Mikolajewicz, U., Monfray, P., Soldatov, V., Spall, S. A., and Stouffer, R.: Response of ocean ecosystems to climate warming, *Global Biogeochem. Cy.*, 18, GB3003, <https://doi.org/10.1029/2003GB002134>, 2004.
- Sarthou, G., Timmermans, K. R., Blain, S., and Tréguer, P.: Growth physiology and fate of diatoms in the ocean: a review, *J. Sea Res.*, 53, 25–42, <https://doi.org/10.1016/j.seares.2004.01.007>, 2005.
- Schmoker, C., Hernández-León, S., and Calbet, A.: Microzooplankton grazing in the oceans: impacts, data variability, knowledge gaps and future directions, *J. Plankton Res.*, 35, 691–706, 2013.
- Scott, F. J. and Marchant, J.: Antarctic Marine Protists, Australian Biological Resources Study, Canberra, 2005.
- Sedwick, P., Blain, S., Quéguiner, B., Griffiths, F., Fiala, M., Bucciarelli, E., and Denis, M.: Resource limitation of phytoplankton growth in the Crozet Basin, Subantarctic Southern Ocean, *Deep-Sea Res. Pt. II*, 49, 3327–3349, [https://doi.org/10.1016/S0967-0645\(02\)00086-3](https://doi.org/10.1016/S0967-0645(02)00086-3), 2002.
- Sigmon, D. E., Nelson, D. M., and Brzezinski, M. A.: The Si cycle in the Pacific sector of the Southern Ocean: seasonal diatom production in the surface layer and export to the deep sea, *Deep-Sea Res. Pt. II*, 49, 1747–1763, [https://doi.org/10.1016/S0967-0645\(02\)00010-3](https://doi.org/10.1016/S0967-0645(02)00010-3), 2002.
- Signorini, S. R., Garcia, V. M. T., Piola, A. R., Garcia, C. A. E., Mata, M. M., and McClain, C. R.: Seasonal and inter-annual variability of calcite in the vicinity of the Patagonian shelf break (38° S–52° S), *Geophys. Res. Lett.*, 33, L16610, <https://doi.org/10.1029/2006GL026592>, 2006.
- Smith, H. E. K., Tyrrell, T., Charalampopoulou, A., Dumousseaud, C., Legge, O. J., Birchenough, S., Pettit, L. R., Garley, R., Hartman, S. E., Hartman, M. C., Sagoo, N., Daniels, C. J., Achterberg, E. P., and Hydes, D. J.: Predominance of heavily calcified coccolithophores at low CaCO₃ saturation during winter in the Bay of Biscay, *P. Natl. Acad. Sci. USA*, 109, 8845–8849, <https://doi.org/10.1073/pnas.1117508109>, 2012.
- Smith, H. E. K., Poulton, A. J., Hopkins, J., and Balch, W. M.: Coccolithophore and diatom cell abundance from the upper mixed layer of the Great Calcite Belt, January–February 2011 in the

- South Atlantic Ocean and February–March 2012 in the South Indian Ocean, <https://doi.org/10.1594/PANGAEA.879790>, 2017.
- Tortell, P. D., Payne, C. D., Li, Y., Trimborn, S., Rost, B., Smith, W. O., Riesselman, C., Dunbar, R. B., Sedwick, P., and DiTullio, G. R.: CO₂ sensitivity of Southern Ocean phytoplankton, *Geophys. Res. Lett.*, 35, 1–5, <https://doi.org/10.1029/2007GL032583>, 2008.
- Tréguer, P., Nelson, D. M., Van Bennekom, A. J., and DeMaster, D. J., Leynaert, A., and Quéguiner, B.: The Silica Balance in the World Ocean: A Reestimate, *Science*, 268, 375–379, <https://doi.org/10.1126/science.268.5209.375>, 1995.
- Tsuchiya, M., Talley, L. D., and McCartney, M. S.: Water-mass distributions in the western South Atlantic; A section from South Georgia Island (54S) northward across the equator, *J. Marine Sys.*, 52, 55–81, 1994.
- Uitz, J., Claustre, H., Gentili, B., and Stramski, D.: Phytoplankton class-specific primary production in the world's oceans: Seasonal and interannual variability from satellite observations, *Global Biogeochem. Cy.*, 24, GB3016, <https://doi.org/10.1029/2009GB003680>, 2010.
- Venables, H. and Moore, C. M.: Phytoplankton and light limitation in the Southern Ocean: Learning from high-nutrient, high-chlorophyll areas, *J. Geophys. Res.*, 115, C02015, <https://doi.org/10.1029/2009JC005361>, 2010.
- Verbeek, J. W.: Recent calcareous nannoplankton in the southernmost Atlantic, *Polarforschung*, 59, 45–60, 1989.
- Winter, A., Jordan, R. W., and Roth, P. H.: Biogeography of living coccolithophores in ocean waters, in: *Coccolithophores*, edited by: Winter, A. and Siesser, W. G., 39–49, Cambridge University Press, Cambridge, 1994.
- Winter, A., Henderiks, J., Beaufort, L., Rickaby, R. E. M., and Brown, C. W.: Poleward expansion of the coccolithophore *Emiliana huxleyi*, *J. Plankton Res.*, 36, 316–325, <https://doi.org/10.1093/plankt/fbt110>, 2013.
- Young, J., Geisen, M., Cros, L., Kleijne, A., Sprengel, C., Probert, I., and Ostergaard, J.: A guide to extant coccolithophore taxonomy, *J. Nannoplankton Res.*, 1, 1–132, 2003.